ANTIOXIDANT AND ANTI-APOPTOTIC DEFENSES IN THE ANOXIA TOLERANT TURTLE, *TRACHEMYS SCRIPTA ELEGANS*

By

Lin Xie

B.Sc. Hebei University (China), 2005

A Thesis submitted to the Faculty of Graduate Studies and Research
in partial fulfillment of the requirements for the degree of

Master of Science

Department of Biology

Carleton University

Ottawa, ON, Canada

Your file Votre référence
ISBN: 978-0-494-33718-9
Our file Notre référence
ISBN: 978-0-494-33718-9

Abstract

The freshwater turtle, Trachemys scripta elegans, utilizes various biochemical adaptations to survive anoxia-reoxygenation cycles without apparent tissue damage. This thesis focused on changes in the expression and regulation of selected enzymes and proteins involved in antioxidant and anti-apoptotic defense in turtle tissues in response to anoxic submergence and reoxygenation recovery. Western blotting showed that levels of the antioxidant enzyme, manganese superoxide dismutase (Mn SOD), were significantly higher ($P<0.05$) in heart and skeletal muscle during anoxia. Among four isozymes of glutathione S-transferase (GST), GST K1 expression level was enhanced in kidney, liver and muscle during anoxia, but remained stable in heart. GSTT1, GSTP1 and GSTM3 were elevated in a tissue-specific manner. Anoxia-induced upregulation of the transcription factor, Nrf2, coupled with translocation of Nrf2 into the nucleus in anoxia, indicated that Nrf2 is probably involved in activating downstream antioxidant genes such as GST. Analysis of antiapoptotic proteins (Bcl-XL, Bcl-2 and Mcl-1) also showed enhanced expression in selected tissues during anoxia exposure whereas the pro-apoptotic protein, Bad, was suppressed via phosphorylation during anoxia in muscle. Levels of bcl-xl mRNA were also quantified to assess the relationship between bcl-xl gene and Bcl-XL protein expression under anoxia. The results indicate that enhancement of antioxidant and anti-apoptotic defenses is an important adaptive mechanism for effectively dealing with low oxygen and oxidative stresses over cycles of anoxia/reoxygenation in turtles.

Acknowledgments

First and foremost, I would like to thank my supervisor Dr. Kenneth B. Storey who accepted me to his Lab. At many stages in my research work I benefited from his teaching, advice and encouragement. His positive outlook and confidence in my research inspired me and gave me scientific confidence. I also sincerely thank Jan Storey, for her excellent editing, insightful suggestions and continuous encouragement with my thesis. I really appreciate to her great help.

I also wish to thank the members of my committee, Dr. Susan Aitken and Dr. Jean-Michel Weber, for their support and valuable suggestions. Thanks also go to the members of the Storey lab for their help, encouragement and scientific discussions, in particular to Mamady, Jeremy, and Anastasia, from whom I have learned invaluable molecular biology techniques.

Finally, I wish to thank my parents for their love and long-distance support throughout my graduate years of study.

Table of Contents

List of Abbreviations

ATP	adenosine triphosphate
ARE	antioxidant response element
ATF	activating transcription factor
Bad	Bcl-2-associated death protein
Bcl-2	B-cell leukemia/lymphoma 2
Bcl-X_L	B cell leukemia/lymphoma xL
BH	Bcl-2 homology
BLAST	Basic Local Alignment Search Tool
BTB	Bric-a-Brac, Tramtrack and Broad
bZip	basic leucine zipper
cDNA	complementary DNA
CDs	coding sequences
cIAP	cellular inhibitor of apoptosis
CNC	cap 'n' collar
COX1	cytochrome c oxidase subunit 1
DCNB	1,2-dichloro-4-nitrobenzene
DEPC	diethylpyrocarbonate
DTT	dithiothreitol
ECL	enhanced chemiluminescence
EDTA	ethylenediamine tetraacetic acid

EMSA	electrophoretic mobility shift assay
EtBr	ethidium bromide
$FADH_2$	reduced flavin adenine dinucleotide
GPX	peroxidase
GR	glutathione reductase
GRP78	glucose regulated protein 78
GST	glutathione S-transferase
HEPES	N- (2-hydroxyethyl) piperazine-N'- (2-ethanesulfonic acid)
HIF-1alpha	hypoxia-inducible factor-1 alpha
HO1	heme oxygenase 1
IAP	apoptosis inhibitory protein
IRES	internal ribosome entry site
kb	kilobase
kDa	kilo Dalton
Keap1	Kelch-like ECH-associated protein 1
Maf	v-maf musculoaponeurotic fibrosarcoma (avian) oncogene family, protein
MAPK	mitogen-activated protein kinase
MCF7	human breast adenocarcinoma cell
Mcl-1	myeloid cell factor-1
MOPS	2- (N- morpholine) proanesulfonic acid

mRNA	messenger RNA
NADH	reduced nicotinamide adenine dinucleotide
NCBI	National Center for Biotechnology Information
ND	NADH-ubiquinone oxidoreductase
NFκB	nuclear factor kappa B
NQO1	NAD(P)H: quinone oxidoreductase-1
Nrf2	nuclear factor-erythroid 2 related factor –2
PAK	P21-activated kinase
PAGE	polyacrylamide gel electrophoresis
PCR	polymerase chain reaction
PKA	Protein kinase A
PMSF	phenylmethanesulfonyl fluoride
Prx	peroxredoxin
PVDF	polyvinylidine fluoride
ROS	reactive oxygen species
rRNA	ribosomal RNA
RT	room temperature (~21°C)
RT-PCR	reverse-transcriptase polymerase chain reaction
SDS	sodium dodecyl sulfate
SOD	superoxide dismutase
TAE	Tris-Acetate-ethylenediamine tetraacetic acid buffer

TEMED	N,N,N',N'-tetramethylethylenediamine
Tris	tris (hydroxymethyl) aminomethane

List of figures

Chapter 1
General Introduction

Environmental stress resulting from variations in oxygen availability

Living animals are constantly faced with various environmental stresses that challenge normal life, such as oxygen limitation, oxidative, very low or high temperatures, water limitation and food restriction (Storey and Storey, 1990). Of these, oxygen variation in the environment is the one that many animals commonly experience, caused either by variations in environmental oxygen supply (e.g. ice-locked ponds, lakes with hypoxic or anoxic water, O_2 depleted sediments) that deny organisms access to oxygen for extended periods of the time or by animal behaviors that interrupt the supply of oxygen (e.g. breathhold diving by lung-breathing animals, aerial exposure of gill-breathers) (Storey, 1996).

Oxygen depletion, leading to hypoxia and then anoxia is rapidly lethal for many species. In humans and most other mammals, oxygen depletion rapidly interrupts ATP production by mitochondria and thereby disrupts the many ATP-utilizing processes in cells. Perhaps the most dramatic effect is the quick loss of membrane potential difference due to a disruption of the normal balance between the opposing rates of ATP-dependent ion pumps versus ATP-independent ion channels (Hochachka and Lutz, 2001; Storey, 2007). This loss of membrane potential difference then results in the breakdown of critical transmembrane ion gradients, a rise in intracellular Ca^{2+} concentrations, a release of excitatory neurotransmitters, and the triggering of multiple dangerous effects on physiological functions including nerve transmission and muscle contraction leading ultimately to death (Fraser *et al.*, 2001).

On the other hand, excess oxygen, or hyperoxia, can result in an overproduction of reactive oxygen species (ROS) by the mitochondrial respiratory chain and other reactions. ROS species including hydrogen peroxide, superoxide, hydroxyl ion and peroxynitrite are highly reactive and can cause damage to cellular macromolecules (nucleic acids, protein and lipids), resulting in metabolic injury or even cell death to animals. Programmed cell death, or apoptosis, is a distinct genetic and biochemical pathway of cell suicide that is essential for normal organismal homeostasis (Danial and Korsmeyer, 2004). A variety of key events in apoptosis focus on mitochondria, such as changes in electron transport, release of cytochrome c, and altered mitochondrial oxidation-reduction state (Takahashi *et al.*, 2004). It has been shown that ROS can directly stimulate the opening of the mitochondrial membrane transition pore and cause mitochondrial depolarization and cytochrome c leakage, which triggers mitochondria-mediated apoptosis (Kang *et al.*, 2002). Furthermore, when ROS production exceeds the antioxidant buffering capacity of a cell, tissue or organ, oxidative stress could occur (Crawford *et al.*, 2000). Oxidative stress has been linked to a variety of pathological conditions including ischemic heart attack, stroke and neurodegenerative diseases in humans (Hermes-Lima *et al.*, 2001).

Hence, to survive environmental stresses such as hypoxia/anoxia and oxidative stress, animals have developed adaptations to deal with the challenges presented by oxygen at physiological, biochemical, and gene levels.

Adaptations to natural hypoxia/anoxia

Although human metabolism is highly oxygen-dependent, many organisms can live without oxygen for extended periods of time, functioning as facultative anaerobes. Several molecular mechanisms are known that contribute to natural hypoxia/anoxia tolerance and these occur widely across phylogeny. These are: (a) accumulation of large glycogen reserves by organs, (b) strategies for buffering or excreting end products to minimize the acidosis that is a consequence of fermentative metabolism, (c) alternative routes of anaerobic carbohydrate catabolism with higher ATP yields compared with glycolysis ending in lactate, (d) good antioxidant defenses to minimize oxidative injury when oxygen is reintroduced, (e) strong metabolic rate suppression to lower ATP needs during anaerobiosis, and (f) enhanced expression of selected genes whose protein products aid anoxia survival (Storey, 2004).

Of these mechanisms, metabolic rate depression has perhaps the greatest impact because it reduces cellular demand for ATP to a level that matches the reduced ATP supply from fermentative pathways of ATP synthesis. This is especially true in some anoxia tolerant vertebrates. For example, freshwater turtles survive long periods of anoxic submergence by lowering their metabolic rate to about 10%-15% of the corresponding aerobic rates at the same temperature (Jackson, 1968). As illustrated in Figure 1.1 for the painted turtle (*Chrysemys picta bellii*) this results in survival times as long as 3 months or more in cold water and is the key to the winter survival underwater by this species (Jackson, 2000). The molecular basis of metabolic rate depression is a

controlled and coordinated reduction in ATP turnover that matches rates of ATP-producing and ATP-consuming processes (Buck and Pamenter, 2006) as well as a reprioritization of ATP use to sustain key cell functions and shut down many nonessential processes while anaerobic (Hochachka and Lutz, 2001). In most cases, the reduced metabolic rate is achieved not only at physiological and biochemical levels (e.g. reduced rates of heart beat and ventilation; coordinated suppression of the activities of ion-motive ATPases and ion channels) but also at the gene/protein expression level where rates of transcription, translation and protein degradation are strongly suppressed during anoxia (Storey, 2007).

Interestingly, however, despite the strong overall suppression of gene expression in anoxic states, anoxia tolerant animals show increased expression of selected genes and the synthesis of specific proteins. Indeed, selective gene expression in response to hypoxia/anoxia enables cells or animals to adapt to the low oxygen condition. These genes and their protein products may act as part of defensive or adaptational mechanisms for cells and animals that deal with hypoxia/anoxia. In mammals, hypoxic treatment leads to the accumulation of hypoxia-inducible factor-1 alpha (HIF-1alpha) which in turn is responsible for the activation of multiple genes (Chávez *et al.*, 2000). Milton *et al.* (2006) found that gene transcription of neuroglobin was upregulated by anoxia in the brain of red-eared slider turtles, which may protect turtle neurons from anoxic insult. Hypoxic regulation of genes that are involved in apoptosis resistance has also been reported; increased transcriptional activity of apoptosis inhibitory protein IAP-2 was seen in rat

kidney proximal tubule cells treated by severe hypoxia (Dong *et al.*, 2001). The molecular mechanisms that govern transcriptional activation under stress conditions are likely mediate by the activation of selected transcription factors which bind to stress response elements present in the promoter region of genes under the transcription factor's control. In addition, posttranscriptional and posttranslational modification, such as increased stability of selected transcripts and proteins, and suppressed protein degradation rate could also result in the upregulation of specific protein products in stressed cells or tissues. Studies of the regulation of anoxia-induced gene expression in anoxia tolerant turtles, the red-eared slider turtles, are part of the focus of my research project.

Adaptive responses to oxidative stress

Potential risks from oxidative stress often accompany hypoxia/anoxia since a burst of ROS is generated when oxygen is reintroduced in the post-hypoxic/anoxic reperfusion phase. Specifically, the electron carriers of the mitochondrial respiratory chain become reduced during hypoxia or anoxia events (Hermes-Lima *et al.*, 2001). The subsequent reintroduction of oxygen after hypoxia/anoxia rapidly reoxidizes these reduced carriers and then causes oxidative stress in cells with an overproduction of ROS (Ruuge *et al.*, 1991). Hence, hypoxia/anoxia tolerant animals should have well-developed antioxidant defenses for dealing with oxidative stress during natural transitions from low to high oxygen availability. In general, two strategies are used. The first is the maintenance of high constitutive antioxidant enzyme systems. For example, studies with

the anoxia tolerant goldfish (*Carassius auratus*) revealed activities of glutathione-dependent antioxidant enzymes such as glutathione S-transferase (GST) and glutathione reductase (GR) that were substantially higher in liver of the goldfish as compared with the activities in other lower vertebrate species (Lushchak *et al.*, 2001; Hermes-Lima *et al.*, 2001). Willmore and Storey (1997a) examined the effect of anoxia/reoxygenation on the antioxidant systems of anoxia tolerant freshwater turtles and found that antioxidant enzyme activities in turtles were frequently in the range of those found in mammals and very much higher than in other cold-blooded lower vertebrates. The second strategy is anoxia/reperfusion-induced enhancement of antioxidant enzymes (Storey, 2007). This has been demonstrated in a variety of lower vertebrates such as leopard frogs and garter snakes. For example, anoxia/recovery treatment resulted in significant enhancements in the activities of muscle and heart catalase and brain GST in leopard frogs (*Rana pipiens*) (Hermes-Lima *et al.*, 2001). Hence, these selective changes to antioxidant defenses might help to minimize oxidative damage during transitions between low and high tissue oxygenation states. Indeed, the use of exogenous antioxidants or the enhanced expression of antioxidant enzymes has been shown to have protective effects in minimizing reoxygenation injuries in human and other mammals (Weisbrot-Lefkowitz *et al.*, 1998; He *et al.*, 2006; Kowluru *et al.*, 2006).

In addition to adjustments of antioxidant defenses to deal with oxidative stress, adaptive responses against cell death are also significant since cycles of hypoxia/anoxia and reperfusion coupled with oxidative stress can lead to severe cell damage and

apoptosis, as introduced before. Substantial evidence has demonstrated that overexpression of antiapoptotic Bcl-2 family members increases cellular resistance to many different death stimuli including oxidative stress and DNA damage in mammals (Jang and Surh, 2004; Saitoh *et al.*, 2003; Yanada *et al.*, 2004). Moreover, studies in our lab on antiapoptotic defenses in wood frogs (*Rana sylvatica*) showed induced expression of several antiapoptotic Bcl-2 family proteins such as Bcl-2, Bcl-X_L by oxidative stress during cycles of freeze/thaw in selected frog tissues. In the present thesis, I explore antiapoptotic systems in anoxia tolerant turtles.

Model animal

The red-eared slider turtle, *Trachemys scripta elegans*, exhibits a remarkable ability to endure prolonged periods of anoxia and is widely used as a model for the study of natural anoxia tolerance and anoxia/reoxygenation survival. Red-eared slider turtles are found throughout the United States east of the Rocky Mountains and into southern Canada (Ernst, 1990). At warm acclimation temperatures (20-25°C), sliders can survive 12-24 h of anoxic submergence, whereas at cold-acclimation temperatures (0-5°C) they can recover physiological functions following 3-4 months of anoxia (Ultsch, 1989). The behavioral responses of *T. s. elegans* to anoxia during months-long winter hibernation at the bottom of ice-locked lakes and rivers display a comatose-like state (Lutz and Nilsson, 1997b). Indeed, such behavior during prolonged winter hibernation without oxygen accompanies a profound ~90% reduction in whole-turtle metabolic rate that greatly slows metabolic fuel use (Jackson, 1968; Jackson, 2000). Another adaptation that is peculiar to

turtles and aids long term anoxia survival is the utilization of bone and shell to store lactate and to buffer the acidity associated with lactate accumulation, thus enabling extremely high concentrations of this glycolytic end product to build up (Jackson, 2000).

Previous studies on turtle adaptations to these stresses mainly focused on physiological and biochemical responses. Physiological adaptations include changes in ventilation and heart rate, alterations in blood composition, altered affinity of hemoglobin for oxygen and so on. Biochemical changes can involve metabolic adjustments such as metabolic rate depression, storage of high reserves of fermentable fuel (glycogen) in all organs, stress-induced modifications of key enzyme activities, etc. (Lutz and Storey, 1997). Recent studies have begun to address stress-induced gene expression that supports anoxia and oxidative stress survival in anoxia tolerant turtles. DNA array screening to assess anoxia-responsive gene expression in brain of *T. s. elegans* showed about 3% of genes was strongly upregulated although expression of the majority of genes was unaltered or suppressed during anoxia (Willmore *et al.*, 2001). Several studies have also revealed some specific genes that are upregulated during anoxia or/and the following aerobic recovery in tissues of red-eared slider turtles (Cai and Storey, 1996; Milton *et al.* 2006; Prentice *et al.*, 2004; Willmore *et al.*, 2001; Storey, 2007). The continual expression of selected genes and synthesis of new proteins in an animal is thought to be important for metabolic regulation and adaptation (Hawkins, 1991).

This thesis focuses on the changes at the gene and protein levels of selected transcription factors, antioxidant-related enzymes, and anti- or pro- apoptotic proteins in

response to anoxia exposure in red-eared slider turtle tissues. In particular, I focus on protein expression of antioxidant and antiapoptotic defenses during anoxia and recovery in heart, liver, kidney and muscle of *T. s. elegans*.

Heart

The heart of red-eared slider turtles is often used as a good model system to examine anoxia/reoxygenation survival adaptations. The cycle of anoxia and reoxygenation in turtle heart is similar to ischemia/reperfusion situation in mammals that is known to occur during heart attack and failure. The turtle heart is very resistant to anoxia, and isolated heart preparations continue to contract under total anoxia for periods of up to 4 hours (Wasser *et al.*, 1990). During prolonged anoxic diving, the heart of the turtle continues to function in order to transport metabolites and waste products among tissues, but cardiac output is greatly reduced in concert with the reduction in whole-animal metabolic rate and the subsequent decreased demand for blood flow (Stecyk and Farrell, 2007). In addition to these physiological adjustments of heart during anoxia, several studies with turtle heart have suggested that transcription of selected genes and gene products that allow the heart to cope with these stresses is also necessary. For example, a cDNA library made from heart of anoxia-treated red-eared sliders showed that two mitochondrially-encoded genes, cytochrome c oxidase subunit 1 (COX1) and subunit 5 of NADH-ubiquinone oxidoreductase (ND5), were upregulated in response to anoxia (Cai and Storey, 1996; Storey, 2007). Furthermore, studies on anoxia-induced gene expression in the heart of another anoxia tolerant turtle, the painted turtle (*C. p.*

marginata) revealed a substantial number of anoxia-responsive genes including genes for antioxidant enzymes that were upregulated in response to anoxia exposure (Storey, 2006a). This result indicates that anoxia could also activate certain antioxidant genes that would deal with potential problems that arise when oxygen returns and metabolic functions increase rapidly again. Such upregulation of antioxidant genes during anoxia may constitute anticipatory adjustments that avoid reperfusion injuries during reoxygenation.

Other tissues

Induction of gene expression by anoxia and reoxygenation also occurs in other tissues of anoxia tolerant turtles. Mitochondrially-encoded genes were also anoxia responsive in liver of red-eared sliders including *cytb* encoding cytochrome b and *nad4* encoding subunit 4 of ND (Willmore *et al.*, 2001). The mitochondrial genes (*cox1* and *nd5*) that were upregulated in turtle heart were also anoxia responsive in skeletal muscle and kidney of *T. s. elegans* (Storey, 2007). The reason for mitochondrial gene up-regulation in anoxic turtle remains to be explored. Notably, however, stress-induced gene expression does not follow set patterns in every turtle tissue but is stress-, tissue- and species-specific (Crawford *et al.*, 2000). This is reasonable as different tissues have different physiological functions. For example, it has been shown that the liver of red-eared slider turtles is particularly important to anoxia tolerance because it is the tissue that has the main stores of glycogen and releases glucose into the blood to supply the fuel to all other organs during anoxic submergence. Turtle tissues such as heart and skeletal

muscle rely heavily on liver-derived glucose when their own glycogen was depleted during anoxia (Warren *et al.*, 2006). Therefore, one would expect that organ-specific changes in activities or/and levels of selected glycolytic enzymes during anoxia in *T. s. elegans*. Indeed, previous experiments have shown organ-specific changes in the kinetic properties of enzymes such as glycogen phosphorylase and phosphofructokinase in tissues of *T. s. elegans* (Brooks and Storey, 1988; Mehrani and Storey, 1995).

Objectives and hypothesis

Chapter 2. Antioxidant regulation during anoxia and aerobic recovery

The tissues of the red-eared slider turtle, *T. s. elegans*, are subjected to low oxygen tensions during breath hold diving and this can even progress to full anoxia during winter hibernation under water. Not only are adaptations needed to support anaerobic survival but other mechanisms are needed when oxygen is reintroduced to limit damage from ROS generation in the reoxygenation phase when normal antioxidant defenses may be overwhelmed. Hence, adaptive changes in antioxidant defenses may be key for anoxia tolerant turtles to survive anoxia and oxidative stress during recovery.

Hypothesis: Anoxia/reoxygenation survival involves adaptations of antioxidant defense systems by upregulating selected genes encoding antioxidant enzymes under the control of a transcription factor such as Nrf2.

Chapter 2 tested this hypothesis by evaluating changes in the protein levels of key antioxidant enzymes, manganese-dependent superoxide dismutase (Mn SOD) and several isozymes of glutathione-*S*-transferase (GST), in selected tissues of anoxia tolerant turtles

using Western blotting. Furthermore, the involvement of the Nrf2 transcription factor in the expression of antioxidant genes was evaluated by quantifying changes in Nrf2 protein levels and the subcellular distribution of Nrf2 between cytoplasmic and nuclear compartments.

Chapter 3. Anti-apoptotic regulation during anoxia/recovery

When dealing with possible anoxia and reperfusion injuries, antioxidant defenses alone are not sufficient. Both oxygen deprivation (hypoxia/anoxia) and ischemia (hypoperfusion of tissues) have been demonstrated to trigger apoptosis in nontolerant species. Presumably, anoxia tolerant species would have mechanisms to prevent cell death under such circumstances. Hence, I predicted that the suppression of stress-mediated apoptosis would be another adaptive mechanism displayed by anoxia tolerant turtles in order to maintain cell and organ during anaerobiosis.

Hypothesis: Apoptosis is suppressed during anoxia/recovery via altered expression of anti-apoptotic and pro-apoptotic proteins in turtle tissues.

Chapter 3 uses Western blotting to analyze the relative levels of three main proteins that have anti-apoptotic functions (Bcl-X_L, Bcl-2, Mcl-1) in red-eared slider tissues. The proapoptotic protein, Bad, was also examined. Transcript levels of *bcl-xl* were also quantified via RT-PCR in heart to determine whether gene regulation was responsible for anoxia-responsive changes in Bcl-X_L protein levels.

Cause and Effect versus Correlation Studies

My research studies were done on tissues isolated from live animals subjected to

whole animal 'stress'. I was not able to do either genetic manipulations (overexpression of a gene, use of RNAi etc.) or use cell lines. The genome sequence of the turtle is virtually unknown, so sophisticated genomic/proteomic analysis is not yet possible for this genera.

What I could accomplish is to measure the relative levels of some proteins and some message RNAs in the turtle comparing control and stress and correlated these changes with the stress in the context of what is known for the pathways in other organisms (mammals, C. elegans, Drosophila etc.) In most cases we have to argue from "analogy" -- comparing the stress of anoxia in turtles where it is natural to the deleterious effects of anoxia on other systems.

In this context, I have tried to draw inferences, which I refer to as "cause and effect" but always with the caveat of not being able to active manipulate my experimental organisms to prove causality. In many cases the reader may put in their own interpretations and think of my work as correlative only.

Figure 1.1. Duration of anoxic submergence at various temperatures from which painted turtles (*Chrysemys picta bellii*) have been observed to recover fully. Data are obtained from Jackson (2000).

Figure 1.1

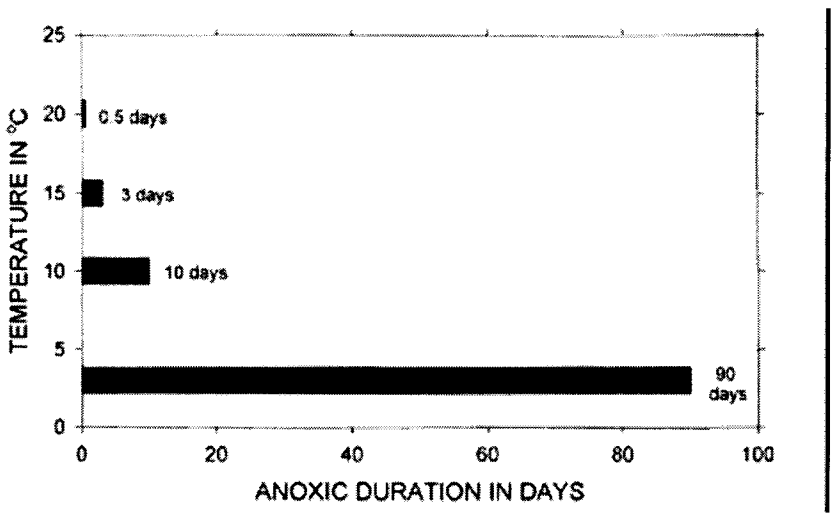

Chapter 2

Expression of the antioxidant enzymes glutathione S-transferases and manganese superoxide dismutase in red-eared slider turtles

Introduction

Anoxia tolerant turtles routinely experience cycles of breathhold diving and aerial breathing during their life. These species can also experience long term submergence for weeks or months during winter hibernation underwater. During prolonged diving under hypoxic or anoxic water, blood oxygen content drops to near zero values (Jackson, 1968). When aerial breathing is restarted, blood oxygen rapidly returns to normoxic levels within the first 10 min of aerobic recovery from anoxia (Willmore and Storey, 1997a). Therefore, tissues of anoxia tolerant turtles experience high natural variation in oxygen availability from anoxia to the following aerial recovery. This situation of deoxygenation-reoxygenation is similar to the states of ischemia-reperfusion that can occur in mammals and lead to serious tissue injury during heart attack or stroke. In the mammalian situation, much of the damage is actually due to oxidative stress arising from an overproduction of reactive oxygen species (ROS) during oxygen reperfusion after ischemia. ROS such as superoxide, hydrogen peroxide, and hydroxyl radical attack biological macromolecules including lipids (peroxidation of unsaturated fatty acids in membranes), proteins (denaturation), carbohydrates and nucleic acids (Blokhida *et al.*, 2003). Anoxia tolerant turtles, however, are able to survive anoxia/reoxygenation cycles without apparent tissue damage. Hence, anoxia tolerant turtles would predictably have efficient antioxidant defenses that deal effectively with the potential for oxidative stress when oxygen is reintroduced to their tissues after extended periods of anaerobic submergence. Indeed, previous studies on antioxidant defenses of anoxia tolerant turtles

in our lab indicated that turtle organs displayed high constitutive antioxidant enzyme activities during anoxia or/and reoxygenation (Willmore and Storey, 1997a). Furthermore, other studies from our lab using cDNA microarray screening to search for anoxia-responsive genes in turtles revealed up-regulation of several genes associated with antioxidant defense during anoxia exposure including *gstm5 & a2, gpx1 & 4, sod1* and *prx1* (Storey, 2006b). Therefore, one of the underlying molecular mechanisms that increase and/or maintain high antioxidant enzyme systems against ROS in turtles could be induction or up-regulation of important antioxidant genes such as glutathione *S*-transferases (GSTs) and superoxide dismutase (SOD) as responses to stress conditions.

The glutathione *S*-transferases (GSTs) are an important family of antioxidant enzymes that catalyze the nucleophilic addition of the thiol of reduced glutathione to a variety of electrophiles (Rushmore and Pickett, 1993). A large number of cytosolic GST isozymes have been purified from mammalian tissues and, on the basis of their primary structures, these have been assigned to five separate families designated class alpha, mu, pi, sigma, and theta GST (Hayes and Pulford, 1995). Evidence suggests that GSTs are inducible following exposure to various stresses such as chemical inducers and oxidative stress (Hayes and Pulford, 1995).

SOD functions efficiently to catalyze the dismutation of the superoxide free radical anions produced in various metabolic processes resulting in the formation of oxygen and hydrogen peroxide molecules ($O2^{-} + O_2^{-} + 2H^{+} \rightarrow H_2O_2 + O_2$) (McCord and Fridovich, 1969). There are two main types of SOD: copper-zinc SOD (CuZn SOD) in cytoplasm

and manganese SOD (Mn SOD) residing in mitochondria (Fridovich, 1995). Of these, mitochondrial Mn SOD should be very important to antioxidant defense of anoxia tolerant turtles since mitochondria are known targets of ROS in ischemia/reperfusion situations. Prolonged anoxia results in the accumulation of reducing equivalents in the cytochrome chain of mitochondria in turtle tissues, and when aerobic recovery starts, ROS are mainly formed from the mitochondria, where electrons are available from the cytochrome chain (Willmore and Storey, 1997a). It has been shown that a stress-induced increase in turtle heart Mn SOD activity occurred during reoxygenation (Willmore and Storey, 1997a).

Regulation of antioxidant enzymes at the transcriptional level is an essential strategy taken to deal with a burst of ROS production and is under the control of specific transcription factors that alter the expression of antioxidant genes in response to oxidative stress. Early experiments suggest that the antioxidant response element (ARE) is an enhancer sequence that mediates transcriptional activation of genes in cells exposed to oxidative stress (Nguyen *et al.*, 2003). Nuclear factor-erythroid 2 (Nrf2) belongs to the Cap 'n' Collar (CNC) family of basic leucine zipper (bZip) transcription factors that can mediate transcriptional activation of antioxidant enzymes via binding to the ARE (Cullinan and Diehl, 2006). This evolutionarily conserved Nrf2/ARE pathway has been found to up-regulate expression of many antioxidant genes under oxidative stress in a variety of organisms. A hypothetical model of the Nrf2/ARE signaling pathway states that in unstressed cells, Nrf2-mediated transcription is inhibited because Nrf2 is maintained in

a latent cytoplasmic complex by virtue of its binding to the Bric-a-Brac, Tramtrack and Broad Complex (BTB) protein, Keap1 (Itoh *et al.*, 1999). Following induction of an oxidative insult, Nrf2 dissociates from the Nrf2/Keap1 cytoplasmic complex resulting in the entry of Nrf2 into the nucleus (Motohashi and Yamamoto, 2004). Once inside the nucleus, Nrf2 has been shown to dimerize with other bZip transcription factors (i.e. Maf, Jun, etc.) and then bind to the ARE to activate the transcription of downstream antioxidant genes that are known to respond to oxidative stress such as the genes for GSTs, heme oxygenase 1 (HO-1) and SOD (Hayes *et al.*, 1999; Chanas *et al.*, 2002.). This model of Nrf2/ARE pathway is summarized in Figure 2.1.

Anoxia tolerant turtles need to deal with the potentially harmful oxidative stress caused by ROS during the anoxia/recovery process. Key antioxidant enzymes that are maintained at high activities and/or enhanced during anoxia and/or recovery act as an important part of the antioxidant defense in anoxia tolerant turtles. Thus, I hypothesized that the expression of GSTs and Mn SOD genes would be enhanced in turtle organs during the anoxia/recovery process in order to help minimize oxidative stress-induced damage. In addition, I hypothesized that the Nrf2/ARE pathway would be the signal transduction mechanism involved in the up-regulation of these antioxidant genes.

The studies in this chapter examine the regulation of protein expression of GST isozymes and Mn SOD in selected tissues of anoxia tolerant turtles. In order to assess whether GSTs and Mn SOD were regulated via the ARE/Nrf2 pathway, the protein expression and translocation of the Nrf2 transcription factor were also studied.

Figure 2.1. Mechanisms of Nrf2 signaling in coordinated activation of ARE-mediated gene expression. Transcriptional activation of ARE-mediated antioxidant defense genes is largely dependent on activation and translocation of Nrf2. The cytoskeleton-associated protein Keap 1 represses Nrf2 and causes localization of Nrf2 in the cytoplasm under normal conditions. ROS produced by oxidative stress release Nrf2 from Keap 1 inhibition and promote nuclear translocation of Nrf2. In the nucleus, Nrf2 heterodimerizes with other family member, binds to the antioxidant response element (ARE) and thereby leads to the expression of genes encoding antioxidant defense proteins. Figure adapted from Giudice *et al.*, 2006.

Figure 2.1

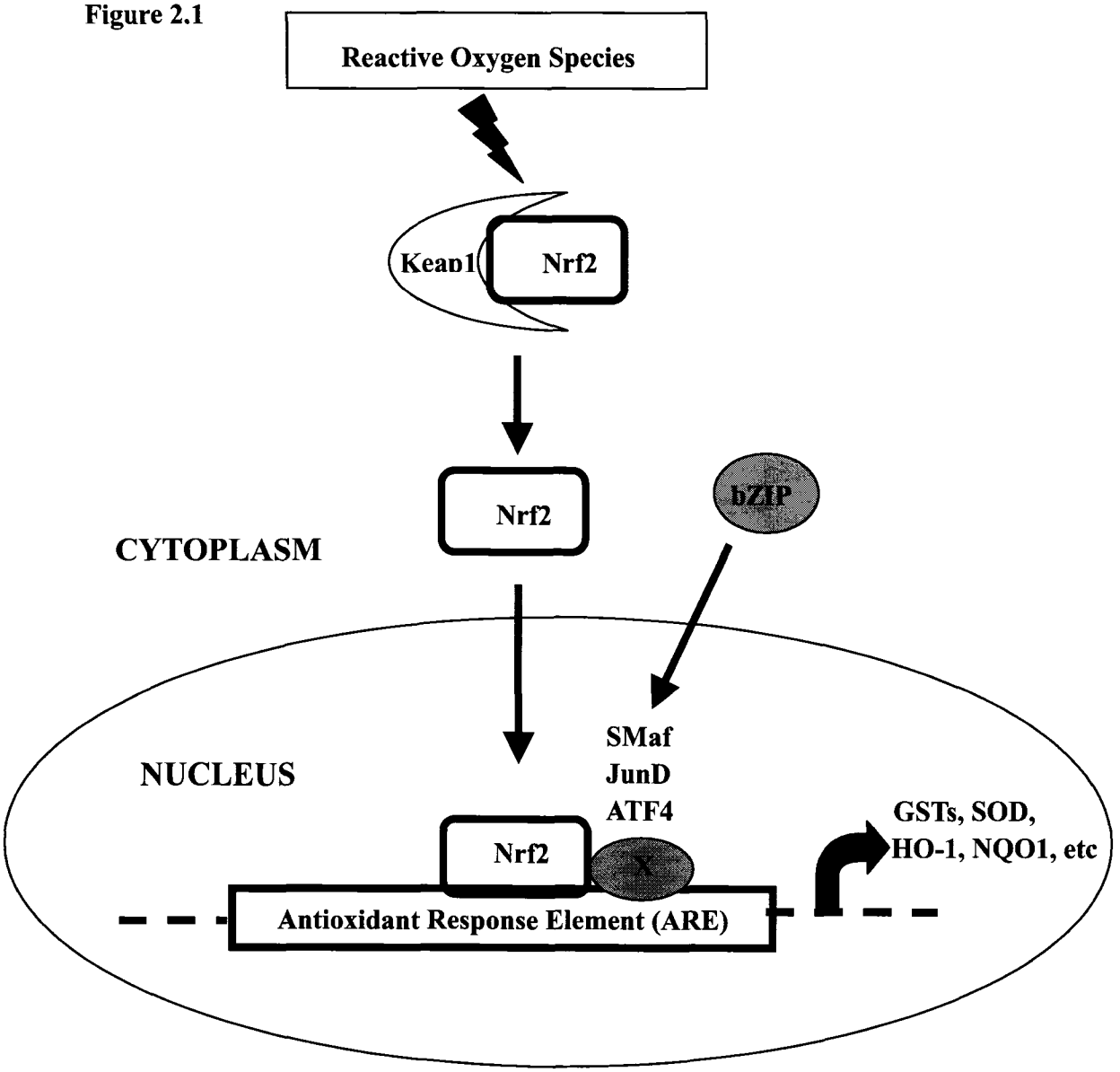

Materials and Methods

Animals

Animal source: Adult red eared slider turtles, (*Trachemys scripta elegans*), were purchased from Wards Natural Science, Mississauga, ON and maintained in large tanks of dechlorinated water at 7°C for at least 3 weeks prior to experimentation. Animals were 17-26 centimeters shell length, 11-15 centimeters shell width (0.5 kilograms) and fed Wardley Reptile Ten Floating Food Stick (New Jersey, U.S.A.) ad libitum. Turtles were provided with a basking platform but no heat lamp. Just prior to experimentation, turtles were transferred a few at a time to the lab in large, covered plastic containers (2 turtles per box, no water added) and were placed in the 5°C fridge for 2 h before experimentation.

Animal treatments: Aerobic control turtles were maintained at 5°C for 2 hours prior to being killed by rapid decapitation. The shells were opened and internal tissues were quickly excised and immediately frozen in liquid nitrogen. Samples were stored at -80°C until use.

Submergence anoxia was imposed by submerging turtles for 20 hours at 5°C in sealed tanks of 40 L deoxygenated water that had been previously bubbled with 100% nitrogen gas for at least 6 hours. Tanks were held in incubators set to 5°C ± 1°C. A wire mesh was fitted about 10 cm below the water line so that turtles could not surface during the deep hypoxia episode. Bubbling with gas was not continued during the experiment. At the end of anoxia treatment, turtles were killed and dissected as above.

Another group of turtles was treated to anoxia exposure as above and then transferred to boxes (two per box) with aerated water (~ 5mm) on the bottom and allowed to recover from anoxia exposure for 5 hours at 5°C. Recovered turtles were then killed and dissected the same way.

Western blotting analysis of MnSOD, GSTK1, GSTT1, GSTP1, GSTM3, and Nrf2

Western blotting was used to examine the levels of MnSOD, GST isoforms and Nrf2 protein in tissue samples from control, 20 h anoxic at 5°C, and 5 h recovered turtles.

Tissue extracts and quantification of protein: Samples of frozen turtle tissues were weighted (~500 mg) and crushed with a mortar and pestle under liquid nitrogen. Soluble protein was extracted by homogenizing in 1 ml of ice-cold buffer containing 20 mM Hepes, 200 mM NaCl, 0.1 mM EDTA, 10 mM NaF, 1mM Na3VO4, 10 mM ß-glycerophosphate and 1 µl of Sigma protease inhibitor using a Polytron homogenizer. A few crystals of phenylmethylsulfonyl fluoride (PMSF) were added immediately prior to homogenization. Samples were centrifuged at 11,000 rpm for 5 min at 4°C in a Biofuge 15 (Baxter Canlab); supernatant was collected.

Protein concentrations in tissue extracts were determined using the Coomassie blue dye-binding method with the BioRad prepared reagent and bovine serum albumin as the standard (Bradford, 1976). The BioRad reagent was diluted 5-fold with distilled water and tissue extracts were diluted 1:60 (v:v). For assay, 10 µl protein samples were added to 190 µl of the diluted reagent in 96-well microplate wells followed by mixing and 5 min

incubation at room temperature (RT) for color development. Absorbance at 595 nm was then measured and protein concentration was determined from a pre-programmed standard curve using BioLinx 2.0 software.

One-dimensional SDS-Polyacrylamide Gel Electrophoresis: In the aim of fixing the final protein concentration of blue homogenates at 5 μg/μl, the concentration of crude white protein extracts were first adjusted to 10 ug/ul and then mixed 1:1 (v:v) with 2x SDS-PAGE sample buffer containing 100 mM Tris-HCl (pH 6.8), 4% w/v lauryl sulphate (SDS), 20% v/v glycerol, 10% v/v β-mercaptoethanol and 0.2% w/v bromophenol blue and boiled for 5 min. Equal amounts of protein from control, anoxic and recovered samples (15-75 μg depending on the experiment) were then loaded into each well of 10 or 12% SDS polyacrylamide gels. Kaleidoscope prestained molecular mass markers (Bio-Rad) were also loaded in one well to estimate the size and positions of sample proteins on the gel. Based on the subunit molecular mass of the protein of interest, proteins were separated using the discontinuous buffer system of Laemmli (1970). Electrophoretic separation was generally carried out in 1X running buffer (3.03 g Tris base, 14.4 g glycine and 1 g SDS per liter, pH ~8.3) at 180 V for ~50 min at RT using the BioRad Mini-PROTEAN 3 System. After electrophoresis, proteins were transferred onto polyvinylidene difluoride (PVDF) membranes (Immobilon-P Transfer Membrane, Millipore Corp., Bedford, MA) by wet transfer with pre-chilled transfer buffer containing 25 mM Tris (pH 8.5), 192 mM glycine, and 20% v/v methanol at 4°C for 100 min at 70V.

Immunoblotting and protein visualization: To prevent non-specific binding, PVDF

membranes were blocked with 5% non-fat milk in TBST (20 mM Tris, pH 7.5, 150 mM NaCl, 0.05% Tween-20) for 30 min at RT. The blots were washed with TBST (5 min x 3) and then incubated with 5 ml TBST buffer containing primary antibody against the protein of interest on a shaking platform at 4°C overnight. The primary antibodies used were rabbit anti-MnSOD at 1:5000 v:v (Stressgen Biotechnologies), rabbit anti-GSTP1, anti-GSTK1, anti-GSTT1, and anti-GSTM3 polyclonal antibodies (gifts from Dr. John Hayes, Biomedical Research Centre, University of Dundee) at 1:1000 v:v and rabbit anti-Nrf2 polyclonal antibody at 1:3000 v:v (Santa Cruz Biotechnology). After incubation with primary antibody, blots were washed with TBST (5 min x 3) and then incubated at room temperature for 2 h with a 1:2000 v/v dilution of secondary antibody, anti-rabbit IgG conjugated to horseradish peroxidase (Cell Signaling). The target protein on the PVDF membrane was detected using an enhanced chemiluminescence (ECL) system (Pierce). The membrane was scanned using ChemiGenius Bio Imaging System (SynGene, Frederick, MD) and the resulting image was analyzed with the associated Gene Tools software. To confirm equal loading in each lane of the blot, total protein on the PVDF membrane was then visualized by staining for 30 min with Coomassie blue solution (0.25% w/v Coomassie Brilliant Blue R, 50 % v/v methanol and 7.5% v/v acetic acid) followed by destaining for 10 min with destain solution (20% distilled water, 20% acetic acid, 60% methanol).

Quantification: Band intensities for the immunoreactive proteins of interest in aerobic control, anoxic and recovered samples were quantified using GeneTools. Intensities of

several Coomassie blue stained "standard" bands (that did not change in intensity between experimental groups) were also quantified in each lane. Normalized band intensities were then determined as the ratio of immunoreactive band intensity versus Coomassie blue band intensity and mean values ± SEM (n=3~5) were calculated for each group. Statistical analysis used the Student's t-test to compare normalized experimental and control values; $P<0.05$ was accepted as significantly different. Data were then plotted as histograms. Error bars shown on the final histograms are SEM values for control, anoxic and recovered trials, respectively.

Analysis of Nrf2 Protein Expression in Nuclear and Cytoplasmic Fractions

Since transcription factors are known to move inside the nucleus where they activate downstream genes, nuclear and cytoplasmic fractions were separated to compare the distribution and translocation of the transcription factor Nrf2 in cytoplasm and nucleus under control, anoxia and recovered conditions.

Briefly, frozen tissues were broken up in liquid nitrogen. Samples were weighed (~0.5 g) and added to 1 ml of 1X homogenization buffer containing 10 mM HEPES, pH 7.9, 10 mM KCl, 10 mM EDTA, 1 mM DTT and 10 µl protease inhibitor cocktail (1 mM PMSF, 0.015% w/v aprotinin, 10 µM leupeptin, 1 µM pepstatin, 1 mM NaF). Samples were homogenized with gentle piston strokes using a Dounce homogenizer and centrifuged at 10,000 x g for 10 min at 4°C. The supernatant representing the cytoplasmic extract was removed into a sterile Eppendorf tube and stored in a freezer at -80°C. The nuclear pellet

was resuspended in 150 µl of 1X extraction buffer containing 20 mM HEPES, pH 7.9, 0.4 M NaCl, 1 mM EDTA, 10 % v/v glycerol, 0.15 mM DTT and 1.5 µl of protease inhibitor cocktail. This resuspension was incubated on ice with gently shaking for 1 h followed by centrifuging at 10,000 rpm for 10 min at 4°C. The second supernatant was saved as the nuclear extract and stored at -80°C. Protein concentration in both the nuclear and cytoplasmic fraction was determined by the Bio-Rad protein assay. Nrf2 protein content in cytoplasmic and nuclear fractions was then assessed using Western blotting, as above.

Results

Mn SOD protein levels in tissues of *T. s. elegans*

Mn SOD protein levels were assessed via Western blotting in four tissues of 5°C aerobic control, 20 h anoxic at 5°C and 5 h recovered *T. s. elegans* (Figure 2.2). The polyclonal human antibody crossreacted with turtle Mn SOD showing a single protein band of ~25 kDa (the expected molecular weight) on immunoblots. Fig. 2.2A shows the full Western blot of Mn SOD protein levels in white muscle (n=5 independent samples from each condition) of adult red-eared slider turtles and Figure 2.2B shows representative cropped blots for the four tissues assessed (n=5 for each condition). Data for multiple trials are summarized in the histogram (Figure 2.2C). During anoxia, Mn SOD protein content was significantly higher ($P<0.05$) in both heart and muscle, by 1.70- and 1.17-fold, respectively, as compared with the corresponding control levels. However, levels reverted to control values after recovery. Mn SOD protein levels did not change

significantly in either liver or kidney during anoxia or recovery states.

Western blotting analysis of GST isoforms in *T. s. elegans*

GST K1 protein levels in tissues of *T. s. elegans*: The effect of 20 h anoxia and 5 h aerobic recovery on GST K1 protein levels was evaluated by Western blotting. The anti-GST K1 polyclonal antibody cross-reacted with a major band on the blots at a molecular weight of ~31 kDa, which is typical for GST K1 enzyme in mammals. Figure 2.3 shows GST K1 protein levels in four tissues of anoxia-tolerant turtles. Figure 2.3A shows a full blot for kidney (n=4 independent samples from each condition) with a protein standard lane whereas Figure 2.3B shows representative cropped blots for each tissue (n=4 for each condition). GST K1 protein content increased significantly in kidney, liver and muscle during anoxia, but remained stable in heart (Figure 2.3C). In kidney, GST K1 rose by 2-fold during anoxia ($P<0.01$) and then returned to control levels during recovery. Liver and muscle showed similar results, GSTK1 increasing significantly ($P<0.01$) by 1.85-fold and 2-fold, respectively, during anoxia and then decreasing to near control levels during recovery.

GST P1 protein levels in tissues of *T. s. elegans:* Western blotting was also used to assess the responses of other GST isoforms to anoxia-recovery. Figure 2.4 reveals the results for GST P1 protein contents in four tissues of turtles. In kidney and heart expression of GST P1 protein did not change over the course of anoxia-recovery. However, in skeletal muscle, protein levels increased significantly ($P<0.05$) by 1.56-fold under anoxic

conditions and remained high during recovery. In liver, protein content remained stable during anoxia, but was reduced significantly ($P<0.05$) during aerobic recovery.

GST T1 protein levels in tissues of *T. s. elegans:* GST T1 protein expression levels in four tissues are shown in Figure 2.5. The levels of GST T1 protein increased significantly ($P<0.05$) by 1.58-fold in liver during anoxia and returned to control levels after anoxia. A similar trend was seen in heart, where protein content also increased significantly ($P<0.05$) by 1.43-fold during anoxia, but was reduced again during aerobic recovery. GST T1 protein levels in muscle were elevated significantly during anoxia by 1.34-fold and increased further to 1.55-fold higher than controls during recovery. Expression levels of GST T1 remained stable in kidney under all three conditions.

GST M3 protein levels in tissues of *T. s. elegans:* GST M3 levels showed no change in kidney or liver during anoxia or recovery (Figure 2.6). In heart, protein content was significantly reduced ($P<0.05$) by 60% during anoxia but rose significantly by 1.57-fold in recovery compared with control. In muscle, GST M3 increased significantly by 2-fold during anoxia and then returned to control levels during recovery.

Nrf2 expression analysis in *T. s. elegans*

Western blotting analysis of Nrf2 in turtle tissues revealed that organ-specific changes in the content of the 57 kDa Nrf2 protein occurred under anoxia and/or recovery from anoxia (Figure 2.7). Nrf2 protein levels increased significantly ($P<0.05$) in heart during both anoxia and recovery by 1.50-fold, and 1.85-fold respectively (Figure 2.7B).

In kidney, levels of the protein decreased to 58% ($P<0.05$) of the control value during anoxia but then rebounded following aerobic recovery. Levels of Nrf2 protein were unaffected by anoxia/recovery in liver. Nrf2 protein was not detected in turtle muscle.

Analysis of nuclear translocation of Nrf2 in liver, kidney, and heart

Transcription factors are active in the nucleus and, therefore, changes in the distribution of the Nrf2 transcription factor between cytoplasmic and nuclear compartments imply stress-induced changes in Nrf2 function. In liver, the amount of Nrf2 in the nuclear fraction increased by 1.97-fold ($P<0.05$) during anoxia and, oppositely, decreased by 80% ($P<0.05$) in the anoxic cytoplasmic fraction (Figure 2.8 A and B). These results indicate that the 57 kDa Nrf2 may have a new distribution in turtle liver cells as a response to anoxia and translocate from the cytoplasm into nucleus during anoxia. In kidney, however, the relative levels of Nrf2 protein were unaltered in both the nucleus and cytoplasm during anoxia (Figure 2.9 A and B). Nrf2 protein levels in the nuclear fraction from heart were significantly increased by 1.65-fold during anoxia as compared with controls ($P<0.05$) but the amount of cytoplasmic Nrf2 remained largely stable between control and anoxic samples (Figure 2.10 A and B).

Figure 2.2. Mn SOD protein expression in four tissues of red-eared slider turtles. (A) A full western blot for white muscle showing the Mn SOD protein band at ~25 kDa in control (C), 20 h anoxic at 5°C (S), and 5 h aerobic recovery (R) samples. This demonstrates that only a single cross-reacting band was present. **(B)** Representative Western blots showing Mn SOD protein band in four tissues from control, anoxic and recovery turtles. **(C)** Histograms showing the relative Mn SOD protein levels in anoxia tolerant turtle tissues. Data are mean ± S.E.M., n= 5 independent trials. * - Values for anoxic or recovery samples are significantly different from the corresponding control values using the two-tailed Student's *t*-test, $P < 0.05$.

Figure 2.2

(A)

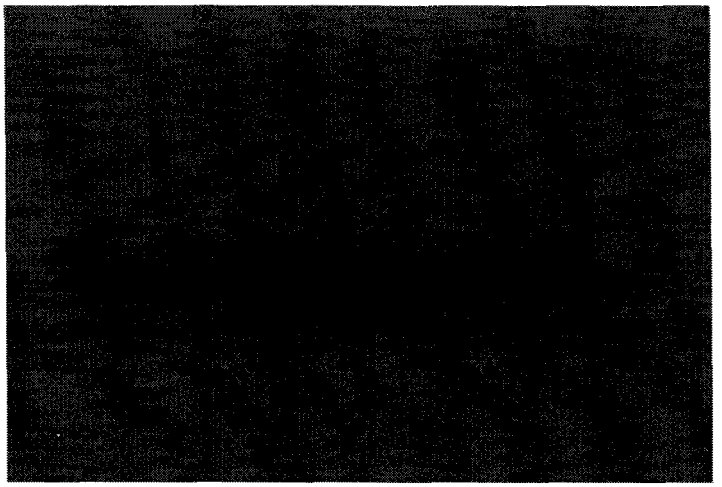

(B)

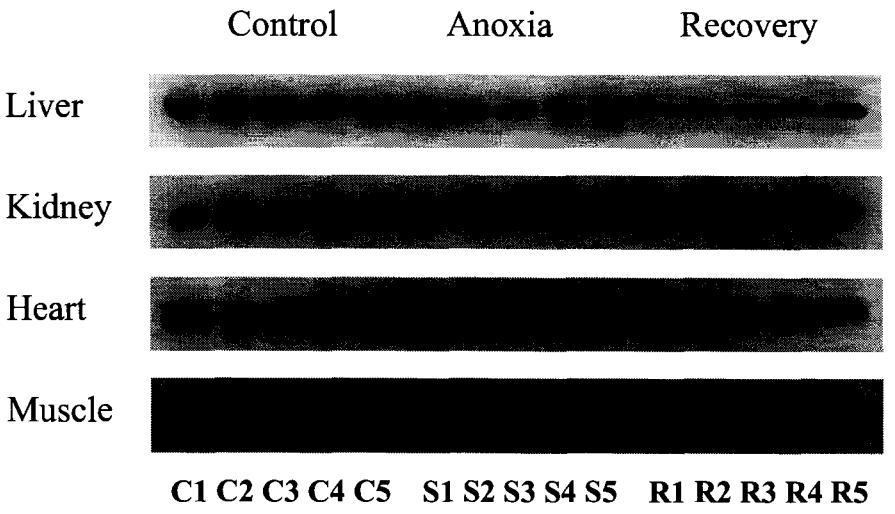

Figure 2.2 continued

(C)

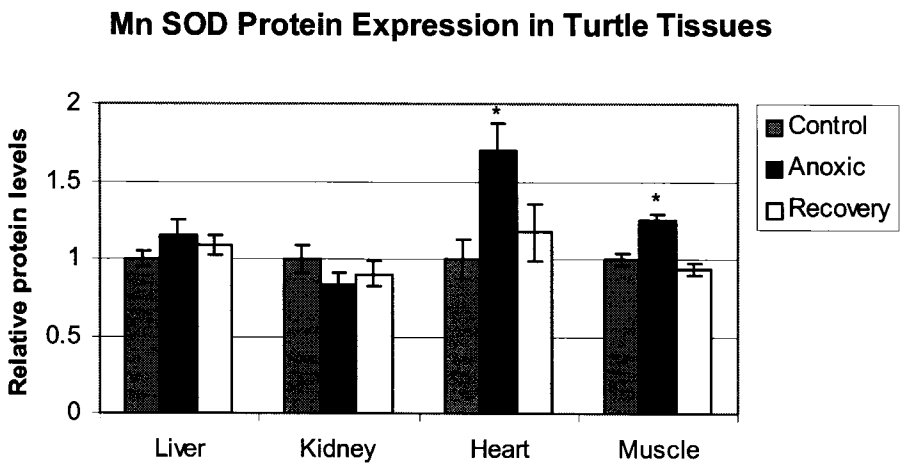

Figure 2.3. GST K1 protein expression in tissues of red-eared slider turtles. (A) A full western blot showing GST K1 protein band at ~31 kDa in kidney of control, 20 h anoxic at 5°C and 5 h aerobic recovery turtles. Four independent samples are shown for each condition: Control (C), lanes 2-5; Anoxic (A), lanes 6-9; Recovery (R) lanes 10-13. A commercial protein ladder (L) from Bio-Rad Laboratories is shown in lane 1 and was used to confirm that the anti-GST K1 antibody crossreacted with a band at the expected size of ~31 kDa. **(B)** Representative Western blots showing GST K1 protein band in four tissues from control, anoxic and recovered turtles. **(C)** Histograms showing the relative GST K1protein levels in anoxia tolerant turtle tissues. Data are mean ± S.E.M., n=4 independent trials. * - Values for anoxic or recovered samples are significantly different from the corresponding control values using the two-tailed Student's *t*-test, $P < 0.05$.

Figure 2.3

(A)

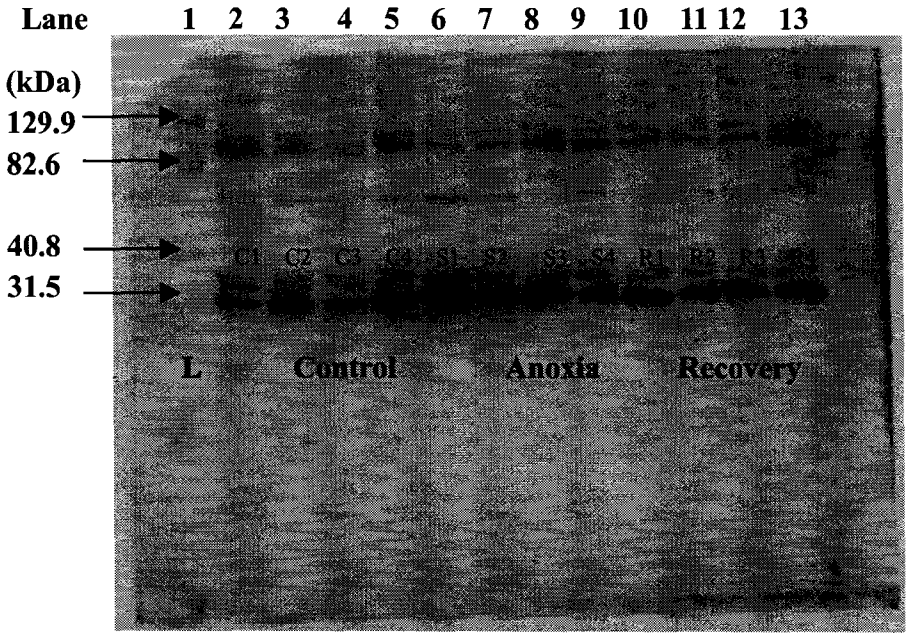

(B)

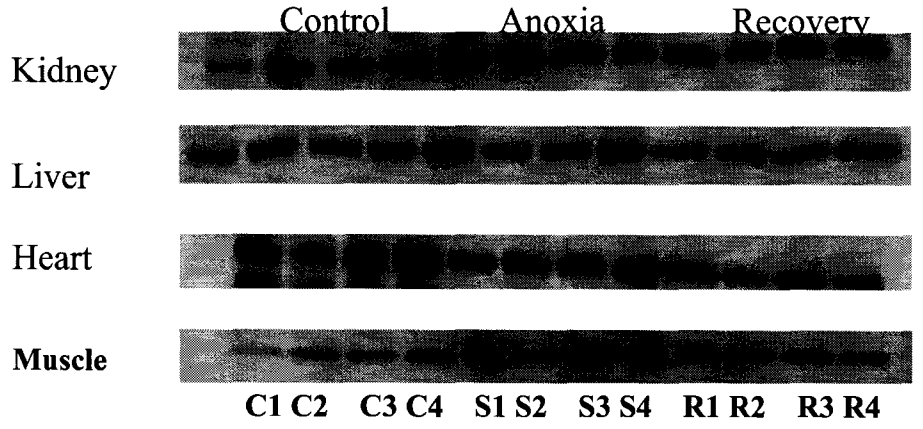

Figure 2.3 continued

(C)

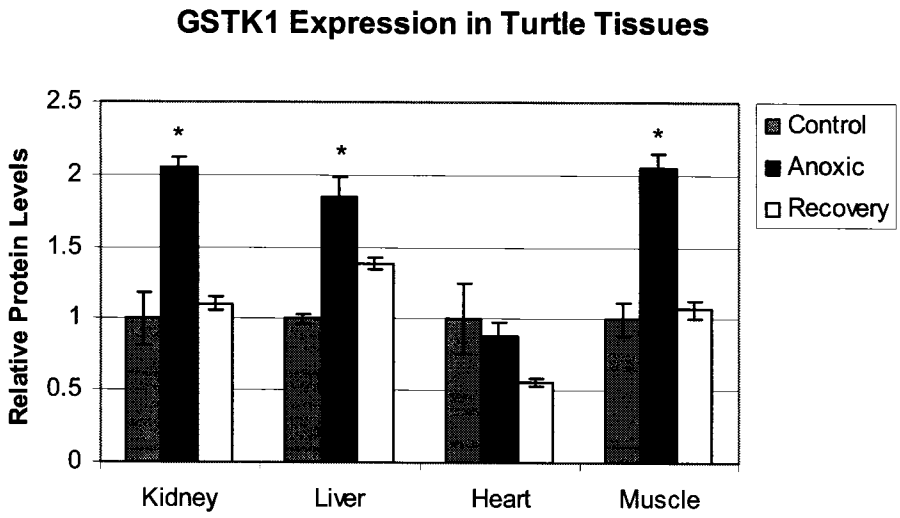

Figure 2.4. GST P1 protein expression in four tissues of red-eared slider turtles. (A) Representative Western blots showing GST P1 protein band in tissues from control, 20 h anoxic at 5°C, and 5 h aerobic recovery turtles. **(B)** Histograms showing the relative GST P1 protein levels in turtle tissues. Data are mean ± S.E.M., n= 4 independent trials. * - Values for anoxic or recovery samples are significantly different from the corresponding control values using the two-tailed Student's *t*-test, $P < 0.05$.

Figure 2.4

(A)

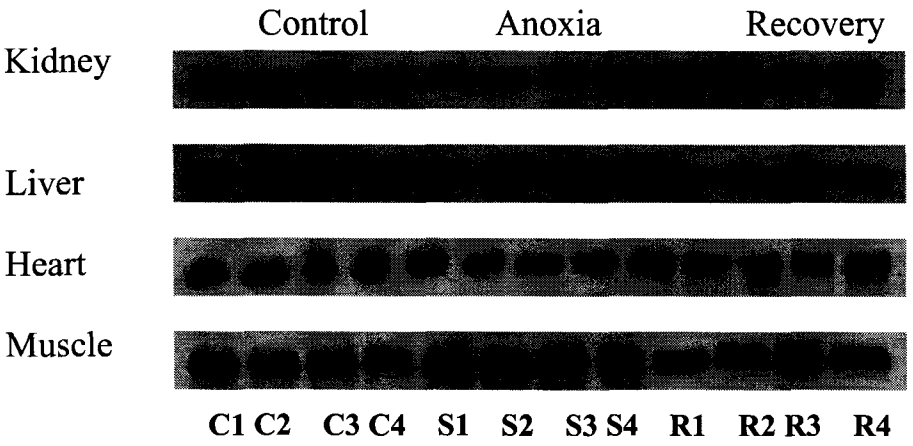

(B)

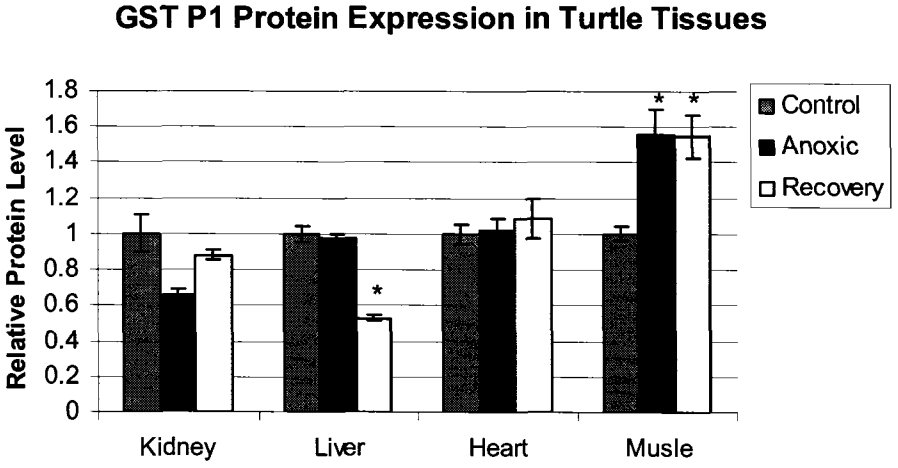

Figure 2.5. GST T1 protein expression in four tissues of red-eared slider turtles. (A) Representative Western blots showing GST T1 protein band in tissues from control, 20 h anoxic at 5°C and 5 h aerobic recovery turtles. **(B)** Histograms showing the relative GST T1 protein levels in anoxia tolerant turtle tissues. Data are mean ± S.E.M., n=3 independent trials for muscle and n=4 for other tissues. * - Values for anoxic or recovery samples are significantly different from the corresponding control values using the two-tailed Student's *t*-test, $P < 0.05$.

Figure 2.5

(A)

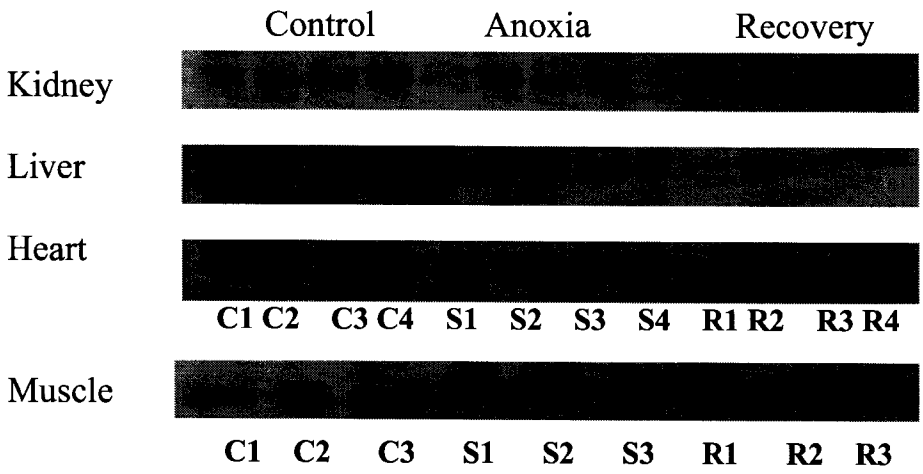

(B)

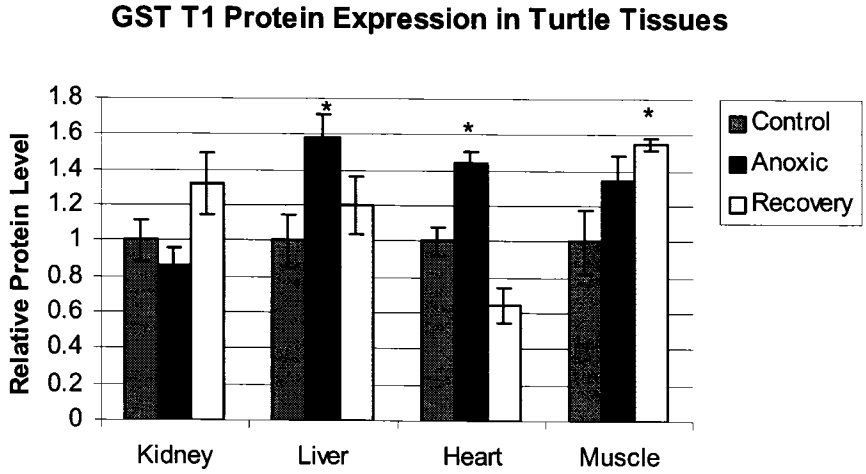

Figure 2.6. GST M3 protein expression in four tissues of red-eared slider turtles. (A) Representative Western blots showing GST M3 protein band in tissues from control, 20 h anoxic at 5°C and 5 h aerobic recovery turtles. **(B)** Histograms showing the relative GST M3 protein levels in anoxia tolerant turtle tissues. Data are mean ± S.E.M., n=4 independent trials. * - Values for anoxic or recovery samples are significantly different from the corresponding control values using the two-tailed Student's *t*-test, $P < 0.05$.

Figure 2.6

(A)

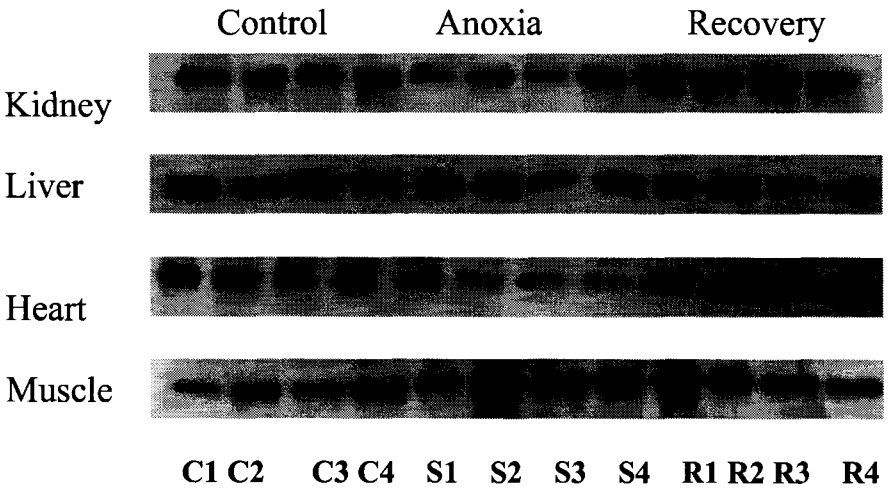

(B)

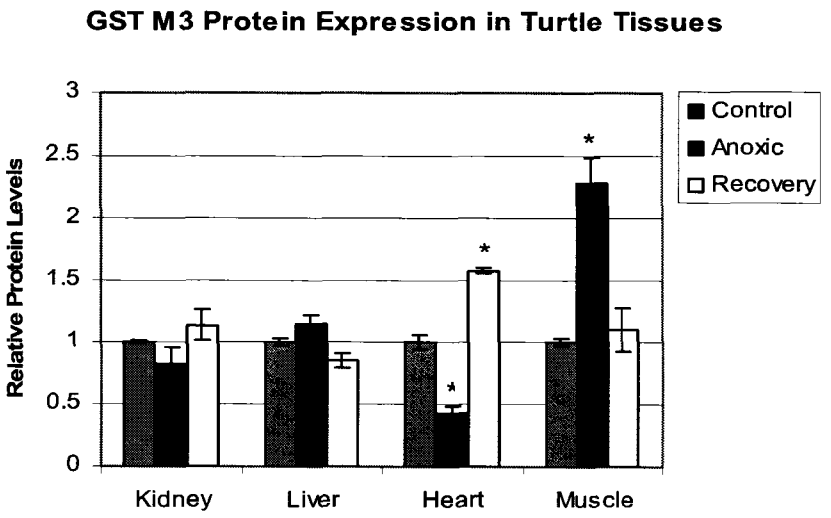

Figure 2.7. Nrf2 protein expression in three tissues of red-eared slider turtles. (A) Representative Western blots showing Nrf2 protein band at ~57 kDa in tissues from control, 20h anoxic at 5°C and 5 h aerobic recovery turtles. **(B)** Histograms showing the relative Nrf2 protein levels in anoxia tolerant turtle tissues. Data are mean ± S.E.M., n = 3 independent trials for heart and n = 4 for other tissues. * - Values for anoxic or recovery are significantly different from the corresponding control values using the two-tailed Student's *t*-test, $P < 0.05$.

Figure 2.7

(A)

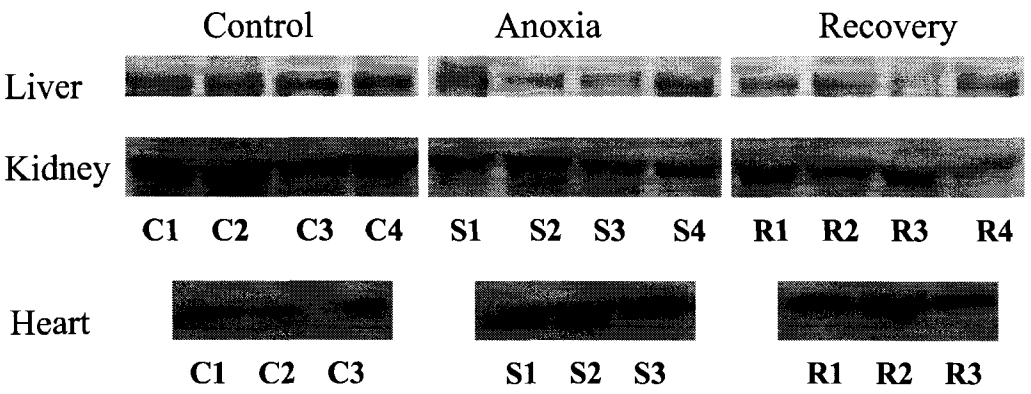

(B)

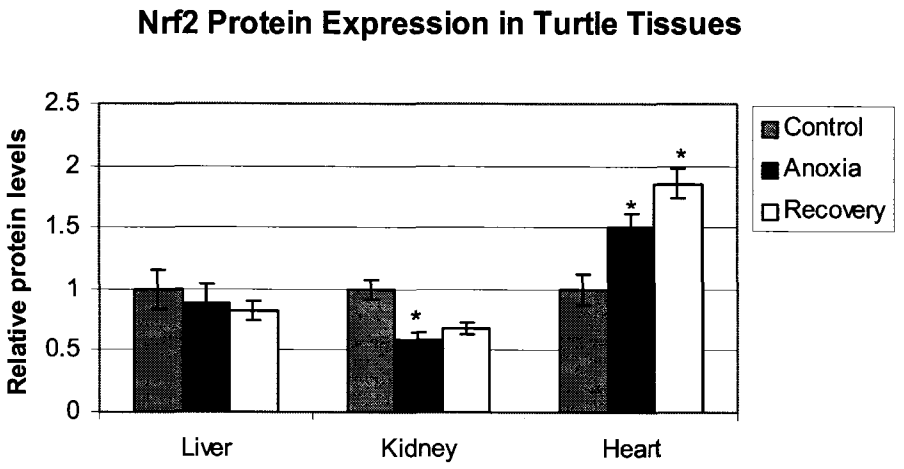

Figure 2.8. Nrf2 protein distributions between cytoplasmic and nuclear fractions of liver in control and 20 h anoxic turtles. Relative protein levels of the anoxic cytoplasmic fraction were compared with that of control cytoplasmic fraction and, likewise, relative protein levels of the anoxic nuclear fraction were compared with that of control nuclear fraction. **(A)** Representative Western blots showing detection of Nrf2 (~57 kDa) in nuclear and cytoplasmic extracts. **(B)** Histograms showing relative levels of Nrf2 in cytoplasmic and nuclear fractions from liver. Data are means ± S.E.M., n = 3 independent trials on different animals. *- Values for anoxic samples are significantly different from the corresponding aerobic control values using the two-tailed Student's *t*-test, $P < 0.05$.

Figure 2.8

(A)

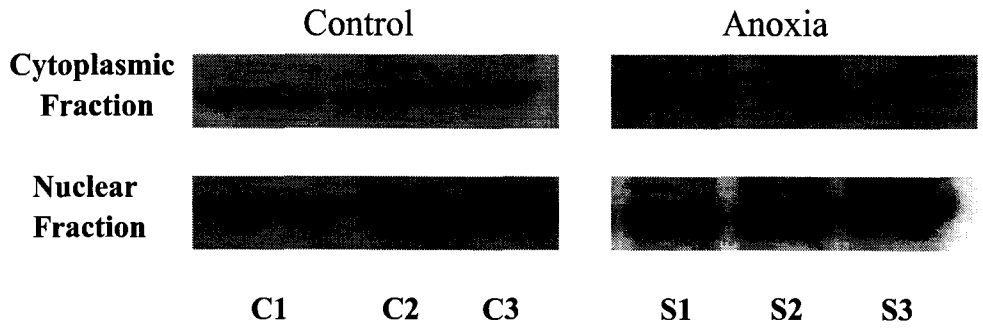

(B)

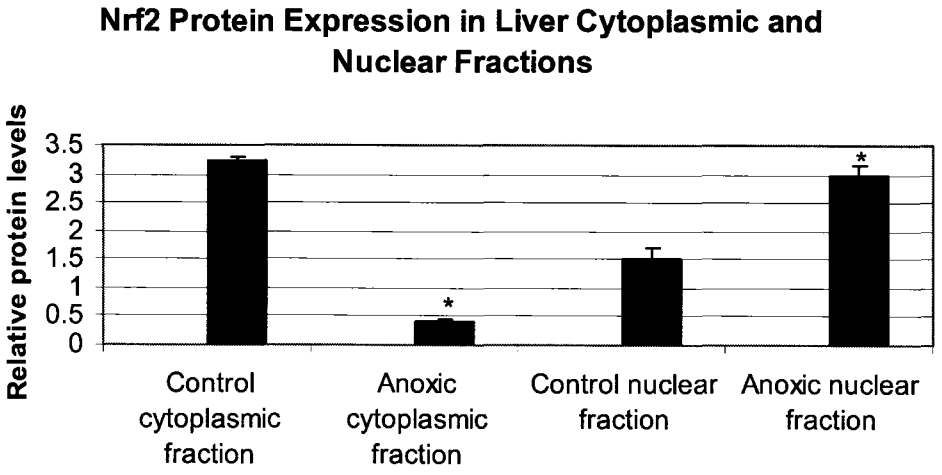

Figure 2.9. Nrf2 protein distributions between cytoplasmic and nuclear fractions of kidney in control and 20 h anoxic turtles. Relative protein levels of the anoxic cytoplasmic fraction were compared with that of control cytoplasmic fraction and, likewise, relative protein levels of the anoxic nuclear fraction were compared with the control nuclear fraction. **(A)** Representative Western blots showing detection of Nrf2 (~57 kDa) in nuclear and cytoplasmic extracts. **(B)** Histograms showing relative levels of Nrf2 in cytoplasmic and nuclear fractions from kidney. Data are means ± S.E.M., n = 4 independent trials on different animals.

Figure 2.9

(A)

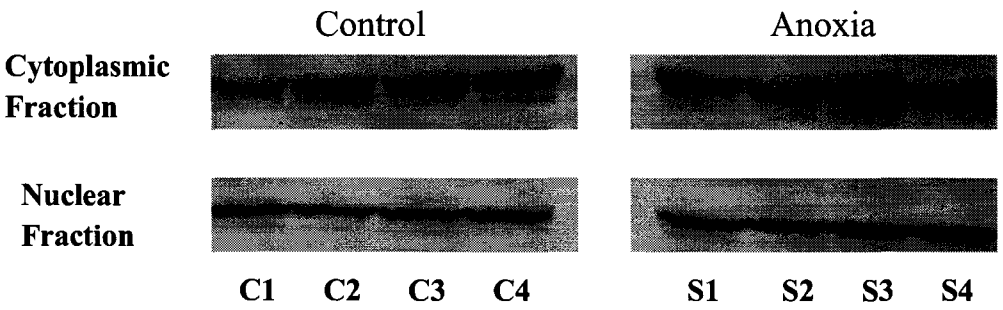

(B)

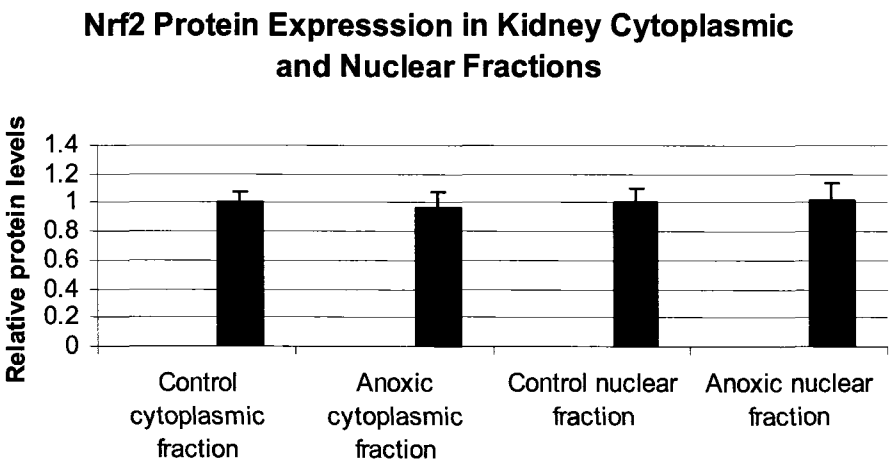

Figure 2.10. Nrf2 protein distributions between cytoplasmic and nuclear fractions of heart in control and 20 h anoxic turtles. Relative protein levels of the anoxic cytoplasmic fraction were compared with that of control cytoplasmic fraction and, likewise, relative protein levels of the anoxic nuclear fraction were compared with the control nuclear fraction. **(A)** Representative Western blots showing detection of Nrf2 (~57 kDa) in nuclear and cytoplasmic extracts. **(B)** Histograms showing relative levels of Nrf2 in cytoplasmic and nuclear fractions from heart. Data are means ± S.E.M., n =4 independent trials on different animals. *- Values for anoxic samples are significantly different from the corresponding control values using the two-tailed Student's *t*-test, $P < 0.05$.

Figure 2.10

(A)

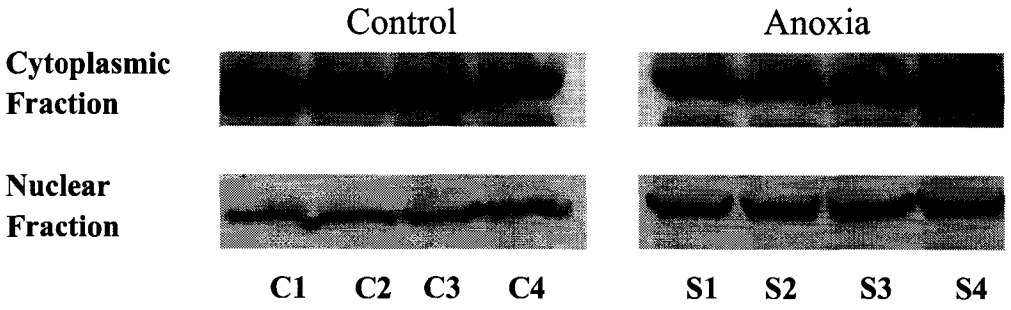

(B)

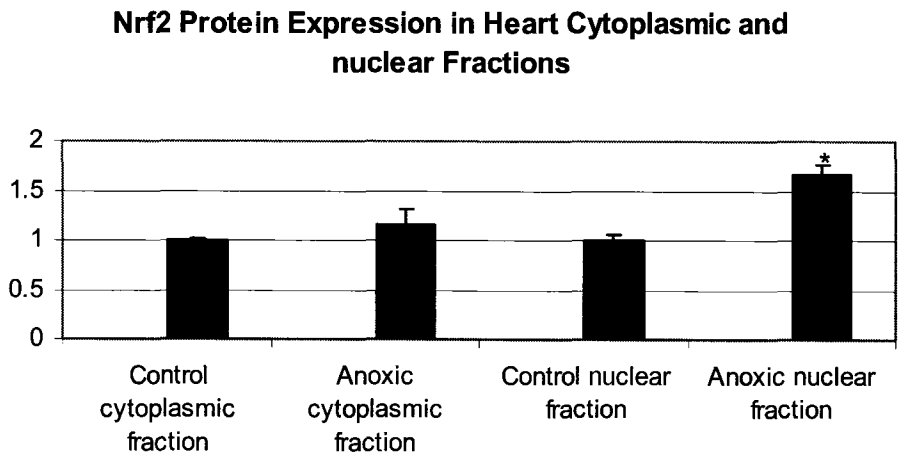

Discussion

Anoxia-tolerant freshwater turtles such as T .s .elegans can survive hours-days of hypoxic breath-hold diving in warm water and several months of hypoxic-anoxic submergence during winter hibernation in cold water (Ultsch 1989). Blood gas analysis has demonstrated that blood oxygen content drops to near 0 Torr by the end of the first hour of anoxic submergence at 24 °C (Jackson 1969). This hypoxia/anoxia results in the accumulation of reducing equivalents (NADH, $FADH_2$) in the cytochrome chain of mitochondria, and when aerobic breathing restarts, ROS are then overproduced from the mitochondria, where excess electrons are available from the cytochrome chain (Willmore and Storey, 1997a). So, anoxia-tolerant turtles need well-developed antioxidant defenses that suit their lifestyle to prevent harmful actions of ROS. Importantly, previous evidence suggested that the increase of ROS formation could also occur in organisms even under hypoxia or anoxia conditions despite the low levels of oxygen (Halliwell and Gutteridge 1999). Palacios-Callender *et al.* (2004) reported an observation of increased superoxide generation in 3% O_2 (hypoxia) treated bovine cells. One possible explanation for this is that the mitochondrial proton leak decreases with low oxygen levels, hence the phosphorylation efficiency is increased, leading to higher superoxide production (Gnaiger *et al.*, 2000). Therefore, the antioxidant defense of turtles could be significant, not only during the sudden reintroduction of oxygen into anoxic tissues with a transient burst of free radicals, but also during potential oxidative stress encountered during the transition into anoxia from normoxic conditions.

Anoxia-tolerant species basically use two strategies for dealing with oxidative stress: (1) high constitutive antioxidant defenses by antioxidant metabolites and enzymes, and (2) anoxia-induced expression of genes encoding antioxidant enzymes (Storey, 2007). While some evidence showed that the tissues of anoxia-tolerant turtles displayed high constitutive antioxidant enzyme activities to prevent cellular damage caused by oxidative stress (Willmore and Storey, 1997a), recent research in our lab has set out to determine whether anoxia-induced antioxidant gene expression and adaptive adjustments also occur in tissues of anoxia-tolerant turtles as responses to anoxia and reoxygenation. DNA array screening to study anoxia-induced gene expression in hatchling painted turtles found that various genes encoding enzymes of antioxidant defense, including isozymes of SOD, glutathione peroxidase, GSTs and peroxiredoxin, were consistently up-regulated in turtle heart and liver (Storey, 2007). Milton and Prentice (2007) also reported a significant increase in SOD transcription during reoxygenation in turtle brain. Hence, accumulating evidence suggests that adaptive regulation of genes encoding antioxidant enzymes plays a positive role in the antioxidant defense of anoxia-tolerant turtles.

Glutathione S-transferases, a group of the most important antioxidant enzymes, are able to catalyze the conjugation of reduced glutathione with various substrates produced by oxidative stress. Once formed, the conjugates can then be exported from the cell by ATP-dependent glutathione S-conjugated efflux pumps (Hayes and Pulford, 1995). In the present chapter, the effect of 20 h anoxic exposure and 5 h aerobic recovery on the regulation of expression of turtle GST isozymes, including GST K1, GST T1, GST P1

and GST M3, was studied by Western blotting. The data for GSTs show that organ-specific changes in the amount or classes of GST isozymes occurred under anoxia and/or recovery from anoxia in turtle tissues. In many times, GST protein content was significantly increased during the 20 h anoxia exposure. For example, turtle GST K1 protein levels (Figure 2.3 C) increase significantly by about 2-fold in kidney, liver and muscle during anoxia whereas GST T1 levels rose significantly in turtle liver, heart and muscle. Both GST P1 and GST M3 were specifically elevated in skeletal muscle under anoxia. These data are consistent with the notion that GST isoforms are differentially expressed in tissue-types in response to anoxia stress, possibly reflecting that individual tissues have unique needs for protection against oxygen stress. Specifically, the importance of GST protection to skeletal muscle is emphasized by the data since the protein content of all four GST isozymes was elevated under anoxia in muscle. The up-regulation of GSTs during anoxia itself is consistent with the notion that there is an anticipatory upward adjustment of the turtle antioxidant defense system in preparation for reoxygenation after anoxia. Furthermore, as mentioned above, evidence showed that oxidative stress could occur in organisms even if the oxygen level is low (hypoxia or anoxia). Therefore, anoxia-induced GST expression may also play a role in dealing with the potential oxidative damage during anoxia in turtle tissues.

Other trends of anoxia-induced up-regulation of GSTs were also observed. In the case of GST K1 in turtle heart, the protein level remained the same during anoxia and recovery compared with control suggesting that induction of GST K1 isoform is not

involved in anoxia/recovery antioxidant defense in turtle heart. It is possible that other GST isozymes or antioxidants other than GST K1 are involved and serve to help improve antioxidant defense of turtle heart since results showed there was a 1.43-fold compensatory up-regulation of GST T1 during anoxia in turtle heart. GST P1 showed up-regulated levels in skeletal muscle during anoxia and recovery. In other turtle tissues, however, GST P1 levels either remained unchanged or decreased after anoxia and recovery treatments. GST P1 is highly efficient in the detoxification of electrophilic alpha, beta-unsaturated carbonyl compounds produced by radical reactions, lipid peroxidation, ionizing radiation, and drug metabolism (Berhane *et al.*, 1994). Similar to GST P1, the GST M3 isozyme was only elevated in anoxic muscle. Interestingly, in heart, protein content of GST M3 was significantly reduced (by 60%) during anoxia but rose significantly (by 1.57-fold) in recovery compared with controls. This suggests that turtle heart GST M3 expression is induced by reoxygenation when more ROS is overproduced rather than anoxia.

Notably, the data showed that each turtle GST enzyme showed different patterns of response both between tissues and as compared with other enzyme family members in the same tissue. Indeed, biological differences in GST induction based on organs, species, age, sex and so on, have been observed previously in mammals. For example, Hayes and Pulford (1995) reported that inducing agents frequently produced a greater increase in GST levels in mouse stomach than in the liver. The different anoxia-induced expression of GSTs in turtle tissues might be due to the different properties of tissues such as their

respective physiological functions, their risk of exposure to oxidative damage, and the balance between synthesis and degradation of proteins during "normal metabolism" (Sani *et al.*, 2006). Furthermore, GST isozymes display marked differences in their ability to conjugate GSH with various electrophiles, which also display selectivity for particular classes of GST isozymes. For instance, 4-hydroxynonenal is selective for GST A4, whereas 1,2-dichloro-4-nitrobenzene (DCNB) is for GST M1 (Hayes and Pulford, 1995). Hence, it could be speculated that different GST isozymes might be needed for removing different oxidative breakdown products caused by oxidative stress in specific turtle tissues.

Cellular defenses against oxidative stresses occurring during anoxia and reoxygenation include both cytosolic and mitochondrial enzymatic antioxidants (Ježek and Hlavatá, 2005). Cytosolic antioxidant defenses include the glutathione S-transferases, as discussed above. A primary mitochondrial antioxidant defenses against oxidative damage is manganese superoxide dismutase (Mn SOD). Mn SOD provides the first line of defense against ROS by dismutation of superoxide at the site of its synthesis. In this study, protein levels of turtle Mn SOD were measured over the anoxia/recovery cycle to see if the enzyme was induced by anoxia and recovery treatments. Western blotting showed that Mn SOD protein content was significantly higher in turtle heart and muscle during anoxia suggesting that anoxia is potent inducer of Mn SOD gene expression in these organs. This again indicates that heart and muscle of anoxia-tolerant turtles increase their antioxidant defenses as an anticipatory response in order to deal with the oxidative

stress that follows prolonged anoxia. These results are consistent with previous evidence showing the role of Mn SOD in mammals. Jones *et al.* (2003) reported that a three-fold up-regulation of Mn SOD activity significantly attenuated myocardial necrosis following induced ischemia/reperfusion in mice. Endurance training also induced Mn SOD expression in rat skeletal muscles (Hollander *et al.*, 1999). These studies indicate that Mn SOD gene expression is activated by a number of stimuli. On the other hand, Mn SOD protein levels did not change significantly in turtle liver and kidney during anoxia and recovery. This may suggest that Mn SOD is not as critical in these organs as it is in muscles and hearts. Alternatively, the constitutive activities of Mn SOD in these organs might be sufficient to deal with any ROS production occurring over anoxia/recovery cycles; further studies to assess Mn SOD activities in these tissues and compare the activities with other organisms would be necessary to evaluate this possibility.

Gene structure analysis of 5'- flanking region of the rat GST Ya subunit gene and the NAD(P)H: quinone reductase gene has demonstrated that a common regulatory element located in the promoters of these antioxidant genes is the antioxidant response element (ARE) (Rushmore *et al.*, 1991). The transcription factor, Nrf2, has been showed to regulate the expression of ARE-containing genes during both basal and stress conditions through translocation to the nucleus and binding to the ARE (Kobayashi *et al.*, 1999). Therefore, it is possible that the inducible regulation of GST and Mn SOD gene expression found in turtle tissues may be correlated with the activation of Nrf2, along with other potential transcription factors that regulate these genes.

In this chapter I looked at Nrf2 relative expression levels during anoxia and recovery and tested the translocation of Nrf2 during anoxia by studying the distribution of the protein between cytoplasmic and nuclear fractions. The results for Nrf2 suggest the possible involvement of Nrf2 / ARE pathway in the induction of GSTs and Mn SOD by anoxia or/and recovery in turtles. Western blot analysis of Nrf2 revealed that levels of the protein increased in heart during anoxia and recovery. This is correlated with the elevated levels of Mn SOD and GST T1 protein in heart during anoxia. Furthermore, Nrf2 protein levels in the nuclear fraction from heart were significantly increased during anoxia. Combined with the observation of the up-regulated expression level of Nrf2 total protein in heart, this further suggests that a high proportion of Nrf2 protein may move to the nucleus, where Nrf2 could bind to ARE to promote more expression of its downstream genes such as *Mn SOD* and *GST T1*. Levels of Nrf2 total protein were unaffected by anoxia/recovery in liver. However, distribution analysis of Nrf2 in liver showed significantly enhanced amount of Nrf2 in the nuclear fraction during anoxia and a decreased amount in the anoxic cytoplasmic fraction. These results imply that Nrf2 protein translocated from liver cytoplasm to the nucleus during anoxia treatment.

In kidney, Nrf2 protein content decreased to 58% of the control value during anoxia. The subcellular distribution of Nrf2 protein in kidney was unaltered in both the nucleus and cytoplasm during anoxia. Hence, taken together, it is possible that other molecular pathways may be involved in the regulation of the anoxia-responsive expression of GSTs and Mn SOD in kidney. Indeed, previous experiments found that an

NF-Kb-like element located in the region of GST P1 promoter appeared to be responsible for regulation of GST P1 expression in human breast adenocarcinoma (MCF7) cells (Hayes and Pulford, 1995). Hussain *et al.* (2004) observed p53-dependent up-regulation of MnSOD transcription in some cell lines. Thus, it could not be ruled out that other *cis*-acting elements in promoter regions of these genes and other transcription factors might be responsible for the regulation of antioxidant responsiveness to oxidative stress in turtle kidney.

In conclusion, these results demonstrated that some GST isozymes were upregulated at the protein level in multiple tissues during anoxia/recovery in anoxia-tolerant turtles. Mn SOD levels were also elevated in heart and muscle during anoxia exposure. The upregulated antioxidant enzymes during anoxia and/or recovery may contribute to minimizing the danger of damage by ROS during transitions between anoxic and aerobic states. In addition, Nrf2 data showed the enhanced level of Nrf2 protein in heart during anoxia/recovery and the translocation of Nrf2 to nucleus in heart and liver. These suggest that the control of GST and Mn SOD expression during anoxia/recovery may be under the regulation of the Nrf2 transcription factor regulating gene expression via the ARE. Further work remains to be done to clarify the precise mechanism of the Nrf2/ARE pathway in turtle tissues.

Chapter 3
Expression of Bcl-2 family proteins and antiapoptotic defense in red-eared slider turtles

Introduction

Apoptosis is a highly controlled process that involves the activation of a genetically determined programmed cell suicide resulting in a morphologically distinct type of cell death characterized by cell shrinkage, nuclear condensation, DNA fragmentation, membrane reorganization, and blebbing (Kerr *et al.*, 1972). There is growing evidence that the induction and regulation of apoptosis is oxygen-dependent, at least in some cases. For example, McClintock *et al.* (2002) observed increased cell death with a decrease in the mitochondrial membrane potential during oxygen deprivation in cultured rat fibroblasts. Magherini *et al.* (2007) reported that hydrogen peroxide (oxidative stress) induced apoptosis in exponentially growing yeast cells. Thus, both oxygen deprivation (hypoxia or anoxia) and oxidative stress can induce apoptosis in a variety of cell types.

Anoxia tolerant turtles naturally encounter high variation in oxygen availability during hypoxic/anoxic diving or hibernation followed by aerial surfacing, which has parallels to ischemia/reperfusion in nontolerant organisms, as discussed in Chapter two. In nontolerant organisms, such anoxia leads to a disruption of ATP production by cellular respiration in mitochondria, which ultimately results in cell death (Brunelle and Chandel, 2002). In addition, oxygen reperfusion causes an overproduction of ROS that has been shown to be inducers or secondary messages of apoptosis (Skulachev, 2000). Therefore, in order to survive natural cycles of anoxia/reperfusion, anoxia tolerant turtles should have regulatory mechanisms that could suppress or override the triggering of apoptosis.

The promotion or inhibition of cell death is regulated by conserved apoptosis

pathways. To date, two major pathways have been identified by which cells can initiate and execute the cell death process: the death receptor pathway and the mitochondrial pathway (Gupta, 2001). The mitochondrial pathway of apoptosis is regulated by the Bcl-2 (B cell leukemia/lymphoma protein 2) family of proteins that is comprised of both antiapoptotic members (such as Bcl-X_L, Bcl-2 and Mcl-1) and proapoptotic members (such as Bad, Bax, and Bak) (Vander and Thompson, 1999). Studies suggest that the complex expression balance and interaction of anti- and pro-apoptotic proteins of the Bcl-2 family regulates the mitochondrial pathway of apoptosis in cells (Gross *et al.* 1999).

Antiapoptotic members of Bcl-2 family such as Bcl-2, Bcl-X_L and Mcl-1 reside in the mitochondrial outer membrane and stop cell death by preventing the loss of outer mitochondrial membrane integrity (Janumyan *et al.*, 2003; Kluck *et al.*, 1997). Evidence shows that enhanced expression of anti-apoptotic proteins could limit apoptosis in cells. For instance, Piret *et al.* (2005) found that overexpression of myeloid cell factor-1 (Mcl-1) protects hypoxic cells against *tert*-butyl hydroperoxide-induced apoptosis. The over-expression of Bcl-X_L also prevented apoptosis due to oxygen deprivation in rat fibroblasts by inhibiting the release of cytochrome c from the mitochondria (McClintock *et al.*, 2002). In addition to modulating the levels of Bcl-2 family members in response to death signals, the function of these proteins can be also regulated by post-translational modification such as phosphorylation. For example, Huang and Cidlowski (2002) reported that the ability of Bcl-2 to inhibit steroid-induced cell death depends on the

phosphorylation status of Bcl-2. Dephosphorylation of Bcl-2 was observed during the induction of apoptosis (Horiuchi *et al.*, 1997) whereas phosphorylation of Bcl-2 at S70 was associated with enhanced antiapoptotic activity in cells (Deng *et al.*, 2004).

Proapoptotic members such as Bad are located in the cytosol and act as sensors of cellular stress and stimuli (Opferman and Korsmeyer, 2003). Bad protein contains 23 serines and 10 threonines within 204 amino acids, and among them, serine 112, 136, and 155 have been identified as phosphorylation sites (Tan *et al.*, 2000; Merighi *et al.*, 2007). In living cells, Bad is phosphorylated by survival factor signaling pathways, including protein kinase A (PKA), protein kinase B (Akt), mitogen-activated protein kinases (MAPKs), or P21-activated kinase (PAK) (Cowan, 2004). Previous data have suggested that phosphorylation of Ser-112 and Ser-136 results in Bad sequestration by cytosolic 14-3-3-family proteins, and thus blocks the apoptotic potentials of Bad by preventing its binding to Bcl-X_L and Bcl-2 on the outer membrane of mitochondria (Figure 3.1) (Hirai and Wang, 2001; Merighi *et al.*, 2007). Once activated by death signaling, Bad is dephosphorylated by calcineurin (PP-2B) or protein phosphatase 1 alpha and relocates to the mitochondrial surface where it forms heterodimers with Bcl-X_L and Bcl-2, reverses their death repressor activity and initiates mitochondrial apoptosis (Figure 3.1) (Hasan *et al.*, 2006).

Tissues of adult red-eared slider turtles (*T. s. elegans*), experience anoxia/reoxygenation without initiating apoptosis. Hence, I hypothesized that altered expression of the anti-apoptotic proteins, Bcl-X_L, Bcl-2 and Mcl-1, and the pro-apoptotic

protein, Bad, may be involved in the adaptive strategy against apoptosis during anoxia and recovery in turtle tissues.

The present chapter uses Western blotting to measure the relative expression levels of antiapoptotic members of Bcl-2 protein family including Bcl-X_L, Bcl-2 and Mcl-1, and examines changes in the amounts of phospho-Bad Ser 112 in selected tissues of control, 20 h anoxic and 5 h recovered red-eared slider turtles. In addition, a partial *bcl-xl* cDNA sequence was amplified and used to quantify transcript levels in turtle heart by RT-PCR. The results suggest that the enhanced expression of anti-apoptotic proteins and the suppression of pro-apoptotic proteins occurs in selected tissues during anoxia and/or recovery and may contribute to the anti-apoptotic defense and cell survival in anoxia tolerant turtles.

Materials and Methods

Animals

Adult red eared slider turtles, *T. s. elegans*, were treated as described in Chapter 2.

Semi-Quantitative RT-PCR analysis of Bcl-xL gene expression

Total RNA Isolation: To prevent RNAase contamination, all materials and solutions used for RNA isolation were treated with 0.1% v/v diethylpyrocarbonate (DEPC) at room temperature (RT, ~21°C) for 12 h and subsequently autoclaved. Frozen tissue samples of ~100 mg were weighed and then homogenized in 1 ml of Trizol™

reagent (Invitrogen) using a Polytron PT1000. After sitting for 5 min at RT, 200 µl of chloroform was added and mixed for 30 s by votex, followed by a further 5 min incubation at RT. Samples were then centrifuged at 11,000 rpm for 15 min at 4°C. The upper aqueous layer containing total RNA was removed and transferred to a DEPC-treated 1.5 ml Eppendorf tube containing 500 µl isopropanol. After gentle shaking, the RNA was precipitated at RT for 10 min. The samples were centrifuged at 11,000 rpm for 15 min to pellet the RNA, the supernatant was discarded and 1 ml of 70% ethanol was used to remove lingering chemicals from the RNA pellet. After centrifugation at 11,000 rpm for 5 min, the supernatant was removed and the final RNA pellet was air-dried for 15 min at RT and then resuspended in 35 µl DEPC-treated water. The quality and quantity of total RNA was judged based from measurements of absorbances at 260 nm and 280 nm (GeneQuant).

In addition, all RNA samples were assessed using 1% agarose gel electrophoresis with ethidium bromide staining to check for the integrity of 18S and 28S ribosomal RNA (rRNA) bands. Briefly, RNA samples were mixed with loading buffer containing 40% w/v sucrose, 0.25% w/v bromophenol blue and 0.25% w/v xylene cyanol FF. Samples were loaded onto 1% agarose TAE gels (1% w/v agarose, 40 mM Tris-acetate, 1 mM EDTA, pH 8.3, 0.0005% v/v EtBr) with 1X TAE running buffer (40 mM Tris-acetate, 1 mM EDTA, pH 8.3) and separated by electrophoresis at 90 V for 45 min. RNA bands was visualized using the UV transilluminator function of the SynGene. High quality of RNA sampled was confirmed by detecting the presence of sharp and distinct 28S and 18S

rRNA bands. RNA samples were stored at -80°C until further use.

First Strand cDNA synthesis: Samples containing 20 μg total RNA were diluted with DEPC water to 10 μl final volume and then 1 μl of 200 ng/μl oligo-dT (5'-TTTTTTTTTTTTTTTTTTTTTTV-3'; V=A or G or C)(Sigma Genosys) was added to each. Sample were then placed in a 68°C water bath for 5 min to denature RNA secondary structure. The mixture was then snap cooled on ice and then 4 μl 5X first strand buffer, 2 μl 0.1 M DTT, 1 μl 10 mM dNTPs and 1 μl M-MLV Reverse Transcriptase (all reagents from Invitrogen) were added; final total volume was 19 μl. The mixture was incubated at 40°C for 60 min and then the cDNA stock was stored at -20°C. Serial dilutions (10^{-1}, 10^{-2}, 10^{-3}, 10^{-4}, and 10^{-5}) of the cDNA stock were prepared in DEPC-treated water and then these were used for PCR amplification.

PCR amplification: Gene specific primers for turtle *Bcl-xL* were designed based on a consensus sequence of *Bcl-xL* derived from the chicken, frog, pig, and rat sequences obtained from NCBI Genbank. Sequences were imported into DNAMAN 4.11 (Lynnon Biosoft) and a multiple sequence alignment was used to identify highly conserved regions of consensus sequence. These were then imported into the Primer Designer program (v.3.0, Scientific and Educational Software) and used to generate both forward and reverse gene-specific primers for *Bcl-xL*. The nucleotide sequences of the *Bcl-xL* primer pairs were: Forward: 5'-GGATACAGCTGGAGTC-3'

Reverse: 5'- ACTACCTGCTCAAAGCTCTG-3'.

The housekeeping gene β-actin was amplified as an internal control; the primers used for

this were: Forward: 5'-CACCAACTGGGACGACATGG-3'

Reverse 5'-GTCGGCCAGCTCGTAGCTCT-3'.

All primers were synthesized by Sigma Genosys and were aliquoted into 300 pmol/µl stocks in DEPC-treated water and stored at -20°C.

For each set of cDNA serial dilutions, two separate PCR reactions were performed, one to evaluate the quantity of the cDNA of interest (*Bcl-xL*) and the other to evaluate the quantity of the housekeeping gene, β-actin. A tube with reaction mix and β-actin primers but with no cDNA was also used as a negative control. The PCR reaction in a 25 µL final volume contained 14 µL of sterile water, 5 µL of diluted cDNA, 1.25 µL 30 nmol/ml forward and reverse primer mixture (1:1), 2.5 µL of 10X PCR buffer (Invitrogen), 1.25 µL of 50 mM $MgCl_2$, 0.5 µL of 10 mM dNTPs and 0.5 µL of *Taq* Polymerase (prepared by the lab of Dr. W. Willmore, Carleton University). The PCR reaction was started with an initial step of 4 min at 94°C followed by 32 cycles of 30 sec at 94°C, 30 sec at 57°C, and 30 sec at 72°C; the final step was 72°C for 7 min. Reactions were performed in a Mastercycler gradient PCR machine (Eppendorf) or an iCycler PCR machine (BioRad). The resulting PCR products were run on 1% agarose/ethidium bromide gels prepared as above, and the single specific cDNA bands of interest at the right position were visualized and quantified using the SynGene.

Quantification: The intensity of the most dilute PCR product that was visible was chosen for quantification purposes to make sure that the products had not become saturated during PCR amplification. This ensures that the final intensity of PCR products chosen for

measuring relative levels of mRNA were proportional to the original amount of mRNA in tissue samples. Quantification of band intensities was performed with the SynGene and the GeneTools program (Syngene, MD, USA). Band intensities for *Bcl-xL* and β-actin were quantified for all samples and the ratio was *Bcl-xL* / β-actin was calculated. Mean normalized band intensities for control, anoxic and recovered samples were then calculated followed by significance testing using the Student's t-test with $P<0.05$ accepted as significantly different.

Sequencing confirmation: RT-PCR products were sequenced by the Ontario Genomics Innovation Centre (Ottawa, ON). Sequences were verified as encoding *Bcl-xL* using the program BLASTN (http://www.ncbi.nlm.nih.gov/blast) at NCBI.

Western blotting

Western blotting was carried out as described in Chapter 2 with aliquots of tissue extracts containing 20-75 μg of soluble protein loaded into wells of 12% SDS-PAGE gels, followed by electrophoresis and transfer to PVDF membranes. Membranes were blocked and washed as described previously and then incubated overnight at 4°C with primary antibody diluted in 1X TBST. The primary antibodies used were rabbit polyclonal antibodies raised against phospho-Stat3 (Tyr705) diluted 1:1000, phospho-Stat3 (Ser727) diluted 1:1000, Bcl-2 diluted 1:500, phospho-Bcl-2 (Ser70) diluted 1:1000, Bcl-xL diluted 1:300, Mcl-1 diluted 1:1000 and phospho-Bad (Ser112) diluted 1: 500 (Cell Signaling Technologies). Secondary antibody (1:2000 v/v dilution) incubations were

carried out for 2 hours at RT and followed by 3 X 5 min washes in 1X TBST. Blots were developed using the enhanced chemiluminescence assay and scanned and analyzed using the SynGene.

Results

cDNA cloning of *bcl-xl* from *T. s. elegans*

Using RT-PCR and primers derived from the consensus sequence of *bcl-xl* from chicken, pigs and house mice, a PCR product of 243 bp was retrieved from total RNA prepared from skeletal muscle of *T. s. elegans*. The nucleotide sequence of the turtle *bcl-xl* fragment and its deduced amino acid sequence are shown in Figure 3.2. The cDNA sequence was verified as encoding *bcl-xl* using the program BLASN at NCBI. The deduced amino acid sequence was also verified to be Bcl-X_L protein by using the program BLASTP at the same site. Figure 3.3 A shows the 235 nucleotide partial cDNA sequence of turtle *bcl-xl* aligned with the corresponding regions of the chicken, pig and mouse nucleotide sequences whose full size coding sequences (CDs) are 690, 702 and 702 nucleotides, respectively. Hence, the turtle sequence represents ~33% of the CDs of the other species. The homology tree in Figure 3.3 B shows that adult turtle *bcl-xl* shares 79% nucleotide identity with the chicken sequence and 66% identity with the pig and mouse sequences over the amplified region.

Figure 3.4 A shows the translated partial amino acid sequence of turtle Bcl-X_L protein aligned with the sequences for the chicken, pig and mouse proteins. The full

Bcl-X_L sequence has 229 residues in chicken, 233 residues in pig and 233 residues in mouse whereas the amplified portion of turtle Bcl-X_L encoded 78 amino acids, corresponding to ~34% of the full sequence. The homology tree (Figure 3.4B) shows that the deduced amino acid sequence of the adult turtle Bcl-X_L protein shared 68% identity with chicken Bcl-X_L and was 57% identical to the mammalian sequences.

Transcript levels of *bcl-xl* in the heart of *T. s. elegans*

The effect of 20 h anoxia and 5 h recovery on *bcl-xl* transcript levels was assessed in turtle heart by semi-quantitative RT-PCR. The housekeeping gene *β-actin* was amplified as an internal control together with the corresponding gene of interest. Figure 3.5 A shows *bcl-xl* mRNA expression in heart together with expression levels of *β-actin*. PCR was conducted using 5 dilutions of cDNA prepared from heart mRNA from control, anoxic and recovered turtles using either *bcl-xl* primers or *β-actin* primers. Transcript levels of *bcl-xl* were then normalized against *β-actin* amplified from the same samples. Figure 3.5 B shows the results from quantifying the bands for three independent trials in turtle heart. The 10^{-3} dilution was chosen to quantify the relative levels of PCR products (representing relative mRNA levels) in the control, anoxia and recovery samples. The result showed that transcript levels were significantly decreased by 63% in turtle heart during anoxia compared with the control and then returned to control levels during recovery.

Western blotting analysis of Bcl-X_L protein levels in turtle heart and muscle

Bcl-X_L protein expression was measured by Western blotting in the heart and white muscle of aerobic control, anoxic (20 h at 5°C) and aerobic recovered (5 h at 5°C) turtles. The Bcl- X_L antibody cross-reacted with a major band at the expected molecular weight of ~30 kDa. Figure 3.6 shows that in heart, Bcl-X_L content increased significantly ($P<0.05$) by 1.57-fold after 20 h anoxia and returned control levels during the aerobic recovery. Bcl-X_L protein levels remained unchanged during anoxia and recovery in skeletal white muscle.

Western blotting analysis of Bcl-2 and phospho-Bcl-2 (ser70) protein levels

Total Bcl-2 protein, as well as the amount of phospho-Bcl-2 phosphorylated on Ser 70, was measured via Western blotting in extracts of liver, kidney, heart and muscle from control, anoxic and recovered turtles (Figure 3.7A and Figure 3.8A). The anti-Bcl-2 and anti-phospho-Bcl-2 (Ser70) polyclonal antibodies cross-reacted with a major band at the expected molecular weight of the protein (~30 kDa). Figure 3.7 B shows that the total amount of Bcl-2 protein did not change during anoxia in liver but it decreased significantly ($P<0.05$) during recovery by 45%. Despite the unchanged total Bcl-2 protein content during anoxia, the level of phosphorylated Bcl-2 (Ser70) in liver rose by 3.45-fold during anoxia ($P<0.05$ compared with control) (Figure 3.8 B). After aerobic recovery, however, the level of phospho-Bcl-2 protein in liver was strongly reduced to just 37% of the control ($P<0.05$). In heart, anoxia treatment did not affect total Bcl-2

content, but recovery caused a significant decrease in the total amount of Bcl-2 protein by 47%. For phospho-Bcl-2 protein expressed in heart, there was no significant difference during anoxia and recovery compared with control. In muscle, the total amount of Bcl-2 protein rose significantly ($P<0.05$) during anoxia by 2.13-fold, but then returned the control level after recovery. A similar expression pattern of phospho-Bcl-2 was observed in muscle where the level of phospho-Bcl-2 increased by 2.99-fold during anoxia ($P<0.05$) and then returned to control levels during recovery.

Western blotting analysis of Mcl-1 protein levels in *T. s. elegans*

The effects of anoxia and recovery on the protein content of another Bcl-2 family member, Mcl-1, were examined in liver, kidney, heart and muscle of anoxia tolerant turtles (Figure 3.9). Initial studies showed that the antibodies crossreacted with only a single band at the expected molecular weight of ~40 kDa for the protein. In liver, Mcl-1 content remained unchanged during anoxia and recovery. Mcl-1 protein showed an interesting expression pattern in kidney by decreasing to 54% of the control level during anoxia followed by increasing strongly by 2.65-fold ($P<0.05$) during aerobic recovery. In heart, the amount of Mcl-1 protein rose significantly ($P<0.05$) during anoxia by 2.13-fold, and remained elevated after recovery. Skeletal muscle protein levels of Mcl-1 were also elevated strongly ($P<0.05$) by 3.09-fold during anoxia and then returned to near control levels after aerobic recovery.

Phospho-Bad (Ser 112) protein levels in *T. s. elegans*

Western blotting was performed to assess phospho-Bad (Ser112) content in some tissues of turtles (Figure 3.10). Although antibody for total Bad protein was tested, it did not crossreact with the turtle protein in any tissue; only the antibody recognizing the phosphorylated peptide (typically a highly conserved sequence) was detectable in turtle extracts. In muscle, the anti-pBad (Ser112) antibody detecting the specific phosphopeptide showed a 1.31-fold ($P < 0.05$) increase in the amount of phosphorylation at Ser 112 during anoxia exposure. However levels of pBad (Ser 112) in liver decreased significantly during anoxia and recovery by 37% and 43%, respectively, compared with controls. Similarly, in kidney, the content of phosphorylated Bad (Ser 112) decreased significantly to 58% ($P<0.05$) of the control value during anoxia and then rose up to 71% of the control after 5 h recovery.

Figure 3.1 In living cells, Bad is phospohrylated by survival factor signaling pathways, which including protein kinase A (PKA), protein Kinase B (Akt), mitogen-activated protein kinases (MAPKs), or P21-activated kinase (PAK). Phosphorylation then results in Bad sequestration by cytosolic 14-3-3-family proteins, and thus blocks the apoptotic potentials of Bad by preventing its binding to Bcl-X_L and Bcl-2 on the outer membrane of mitochondria. Once activated by death signaling, Bad is dephosphorylated by calcineurin (PP-2B) or protein phosphatase 1 alpha and relocate to the mitochondrial surface where it forms heterodimers with Bcl-X_L and Bcl-2, reverses their death repressor activity and initiates mitochondrial apoptosis.

Figure adapted from Cowan, 2004.

Figure 3.1

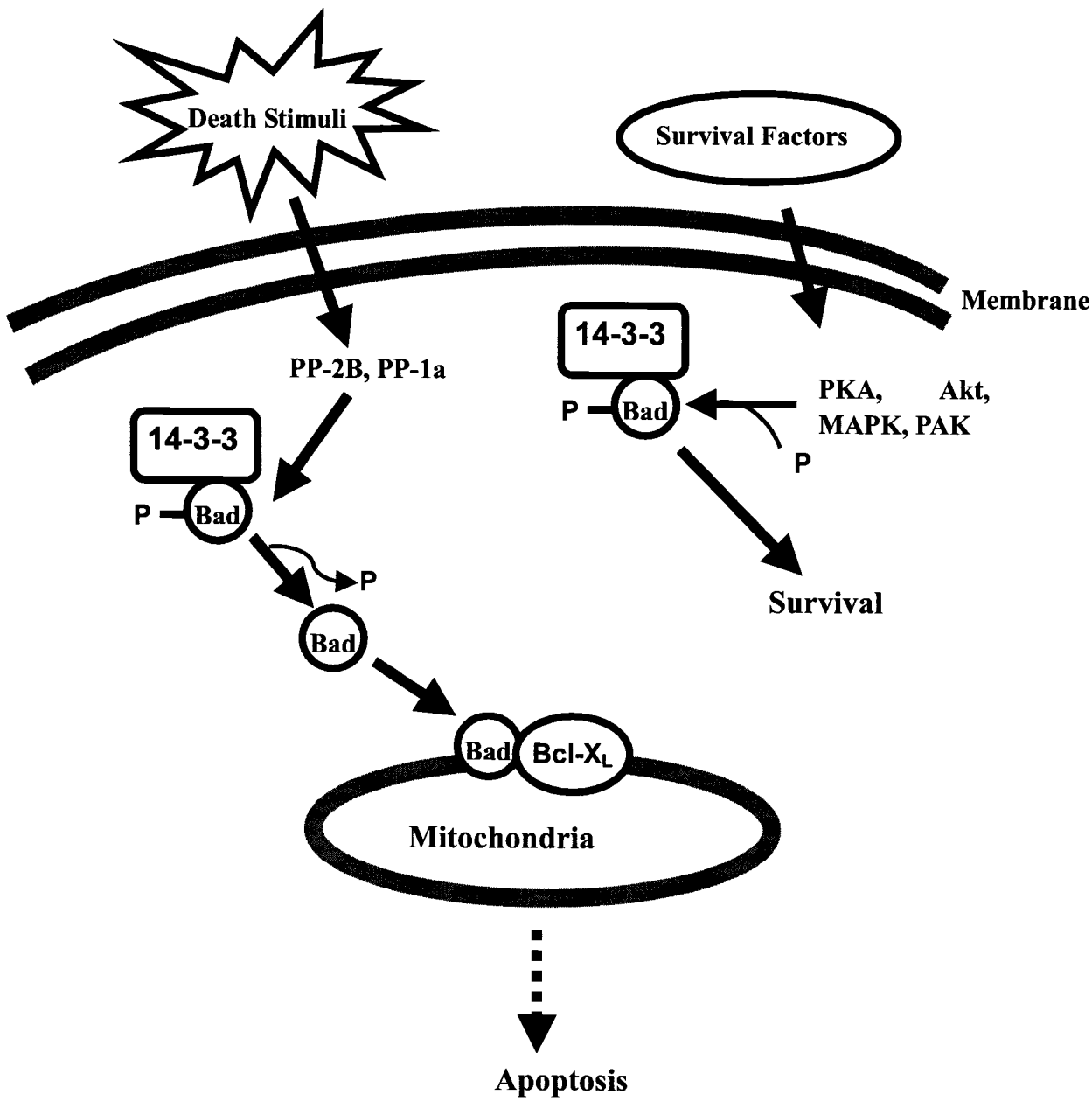

Figure 3.2 Partially amplified *bcl-xl* cDNA sequence and deduced amino acid sequence of Bcl-X_L from white skeletal muscle of red-eared slider turtles (*T. s. elegans*). Nucleotides and amino acids are numbered on the left. A single open reading frame was predicted from the nucleotide sequence and coded for a polypeptide with 78 residues.

Figure 3.2

```
1          GAGTCGGTTCGAGGGGGAGGATGAGATCAGGACTGAGTCTGCAGAAGAGGCTGAGATGGC
1            S  R  F  E  G  E  D  E  I  R  T  E  S  A  E  E  A  E  M  A

61         AAGCGTCCCTAATGGGAGTCCATCCTGGCACCCGGGTGCCAGCCACGTGGTGAATGGGGC
21           S  V  P  N  G  S  P  S  W  H  P  G  A  S  H  V  V  N  G  A

121        TGCCGGGCACAGTAACAGCCTTGAAGCCCATGAAAGGGTTCCGGCAACTGGAGTGAGGCA
41           A  G  H  S  N  S  L  E  A  H  E  R  V  P  A  T  G  V  R  Q

181        GGCACTGAGAGAGGCAGGAGATGAGTTTGAATTGAGGTATTCGGAGGGCTTTCAG
61           A  L  R  E  A  G  D  E  F  E  L  R  Y  S  E  G  F  Q
```

Figure 3.3 (A) The cDNA sequence of *bcl-xl* from red-eared slider turtle (*T. s. elegans*) aligned with nucleotide sequences of chicken (*Gallus gallus*), pig (*Sus scrofa*) and house mouse (*Mus musculus*) (Genbank accession numbers: NM_001025304, AF216205 and NM_009743, respectively). Dashes (-) represent nucleotides in the chicken, pig and house mouse sequences that are identical with the turtle sequence; spacer dots are inserted when nucleotides are not present in all sequences. **(B)** Homology tree of partial turtle, chicken, pig and house mouse nucleotide sequences showing the percent identities.

Figure 3.3

(A)

```
Turtle Bcl-XL       GAGTCGGTTCGAGGGGGAGGATGAGATCAGGACTGAGTCTGCAG......AAGAGGCTGA   60
Chicken Bcl-XL      ---cga-c-g----aa----------a---------ca------......ct-----a--   60
Pig Bcl-XL          -----a---tact-at-t---a----a---a------g-cc---aagggact--at-a--   60
House mouse Bcl-XL  -----a---tagt-at-tc--a----at---------g-cc---aagaaact--a--a--   60

Turtle Bcl-XL       GATGGCAAGCGTCC......CTAATGGGAGTCCATCCTGGCACCCGGGTGCCAGCCACGT  108
Chicken Bcl-XL      -----ac-------......tc--------c--------------ccc----g-------  108
Pig Bcl-XL          agc--a--c-cctagtgccatc-----c-ac-------------t--cg-a-----c--c  120
House mouse Bcl-XL  --g--ag-c-cc-agtgccatc-----c-ac-------------t--cg-at----cg-c  120

Turtle Bcl-XL       GGTGAATGGGGCTGCCGGGCACAGTAACAGCCTTGAAGCCCATGAAAGGGTTCCGGCAAC  168
Chicken Bcl-XL      a-----c--a--ca---t----c-g-g------g----tt-------tt----ga---t-  168
Pig Bcl-XL          ---------a--ca-t--c-----c-g----t-g--t----gg--ggt-a-c--catgg-  180
House mouse Bcl-XL  c--------a--ca-t--c-----c-g---tt-g--t--g-gg--ggt-a----catgg-  180

Turtle Bcl-XL       TGGAGTGAGGCAGGCACTGAGAGAGGCAGGAGATGAGTTTGAATTGAGGTATTCGGAGGG  228
Chicken Bcl-XL      c-ac----------g--------t--g--g----------gc-------c.-------  227
Pig Bcl-XL          --c-----a---a--g-----g-----g--c----------c-------ccg-ag--c  240
House mouse Bcl-XL  --c-----a---a--g-----g-----g--c----------c-------ccg-ag--c  240

Turtle Bcl-XL       CTTTCAG     235
Chicken Bcl-XL      -------     234
Pig Bcl-XL          a--cagt     247
House mouse Bcl-XL  g--cagt     247
```

(B)

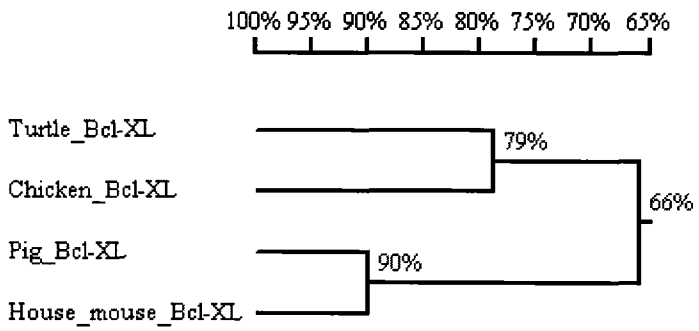

Figure 3.4 (A) Bcl-X_L partial amino acid sequence from red-eared slider turtle (*T. s. elegans*) aligned with chicken (*Gallus gallus*), pig (*Sus scrofa*) and house mouse (*Mus musculus*) sequences (Genbank accession numbers: NP_001020475, NP_999450 and NP_033873, respectively). A highly conserved amino acid region in the turtle sequence, the BH3 domain, is indicated in bold underline. Dashes (-) represent amino acids in the chicken, pig and house mouse sequences that are identical with the turtle sequence; spacer dots are inserted when amino acids are not present in all sequences. **(B)** Homology tree of partial turtle, chicken, pigs and house mice amino acid sequences showing the percent identities.

Figure 3.4

(A)

```
Turtle Bcl-XL          SRFEGEDEIRTESAE....EAEMASVPNGSPSWHPGASHVVN     38
Chicken Bcl-XL         -el-e---n--dt-a....----d--l--------p-g----     38
Pig Bcl-XL             -q-tdve-n---ap-gtes---tp-ai--n----lad-pa--     42
House mouse Bcl-XL     -q-sdve-n---ap-etea-r-tp-ai--n----lad-pa--     42

Turtle Bcl-XL          GAAGHSNSLEAHERVPATGVRQALREAGDEFELRYSEGFQ      78
Chicken Bcl-XL         --tv-rs---v--i-r-sd------d---------rra-s      78
Pig Bcl-XL             --t---s--d-r-vi-maa-k--------------rra-s      82
House mouse Bcl-XL     --t---s--d-r-vi-maa-k--------------rra-s      82
```

(B)

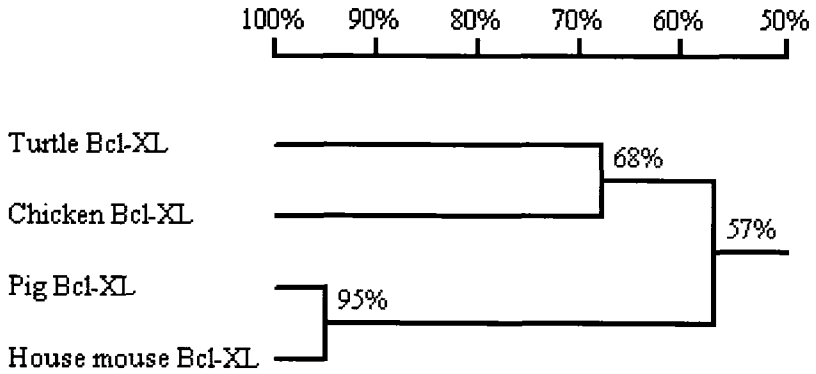

Figure 3.5 Analysis of *bcl-xl* transcript levels in red-eared slider turtle heart by RT-PCR. **(A)** Representative RT-PCR of *bcl-xl*, relative to β-399 in a serial dilution of heart cDNA from control, anoxic and recovery samples. **(B)** Relative *bcl-xl* mRNA levels in heart of turtles from three conditions: control (5°C), anoxia (20 h at 5°C) and aerobic recovery (5 h at 5°C after 20 h anoxia) as determined by RT-PCR. The 10^{-3} dilution was quantified for the histogram. Histogram shows mean ± SEM, n=3 independent determinations. *- Values for anoxic samples are significantly different from the corresponding control values using the two-tailed Student's *t*-test, $P < 0.05$.

Figure 3.5

(A)

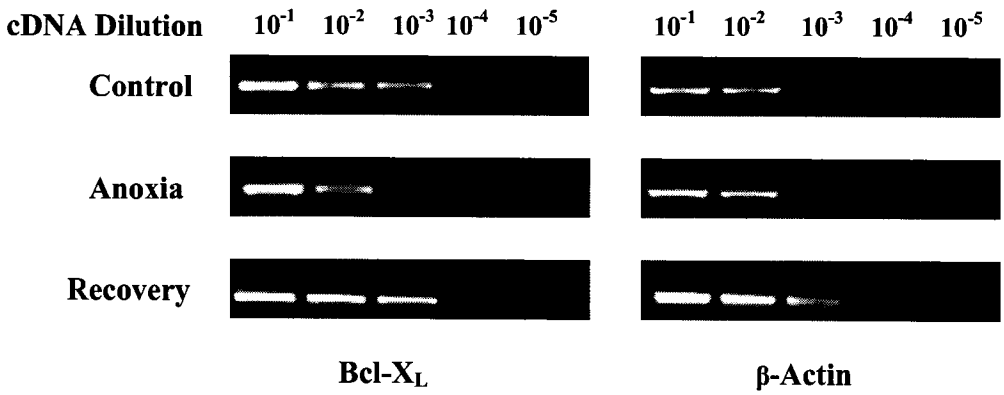

(B)

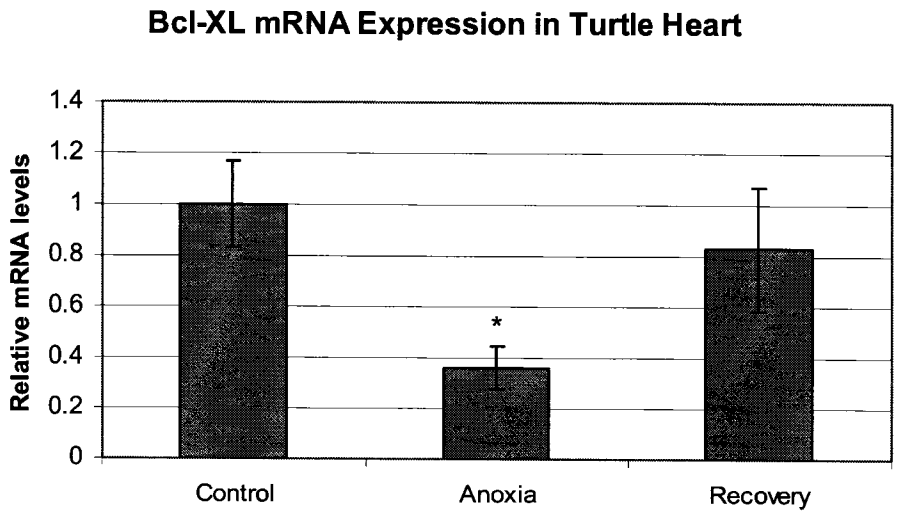

Figure 3.6 Western blots analysis of Bcl-X_L protein content in heart and skeletal muscle of red-eared slider turtles from three conditions: control (5°C acclimated), anoxia (20 h at 5°C) and aerobic recovery (5 h at 5°C after 20 h anoxia). **(A)** Representative Western blots showing the Bcl-X_L protein band at ~30 kDa in tissues of control, anoxic and recovered turtles. Protein bands were normalized against Coomassie stained bands. **(B)** Histograms showing the relative Bcl-X_L protein levels in turtle tissues. Data are mean ± SEM, n= 4 independent trials. * - Values for anoxic samples are significantly different from the corresponding control values using the two-tailed Student's *t*-test, $P < 0.05$.

Figure 3.6

(A)

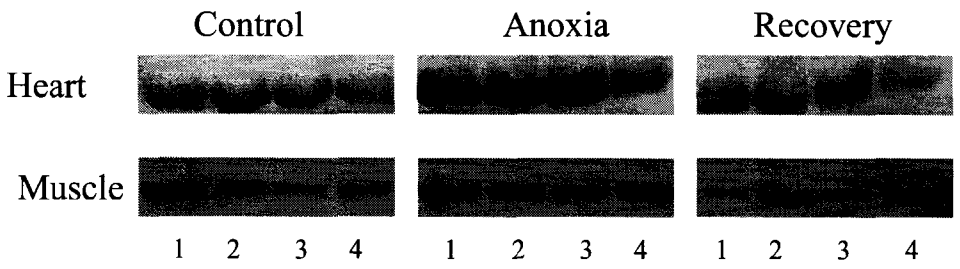

(B)

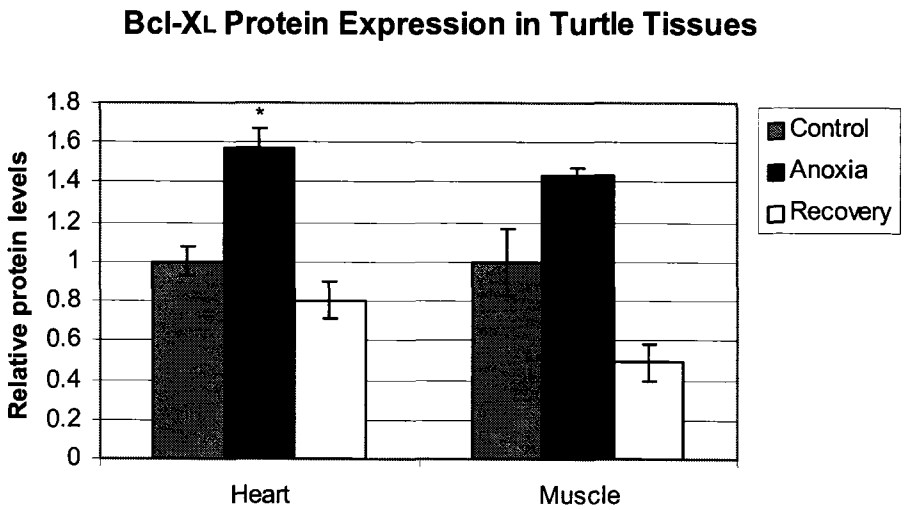

Figure 3.7 Bcl-2 protein expression in three tissues of red-eared slider turtles. **(A)** Representative Western blots showing the Bcl-2 protein band at ~30 kDa in tissues of control, anoxic and recovered turtles. Protein bands were normalized against Coomassie stained bands. **(B)** Histograms showing the relative Bcl-2 protein levels in turtle tissues. Data are mean ± SEM, n= 4 independent trials for liver and muscle and n=3 for heart. * - Values for anoxic or recovery samples are significantly different from the corresponding control values using the two-tailed Student's *t*-test, $P < 0.05$.

Figure 3.7

A)

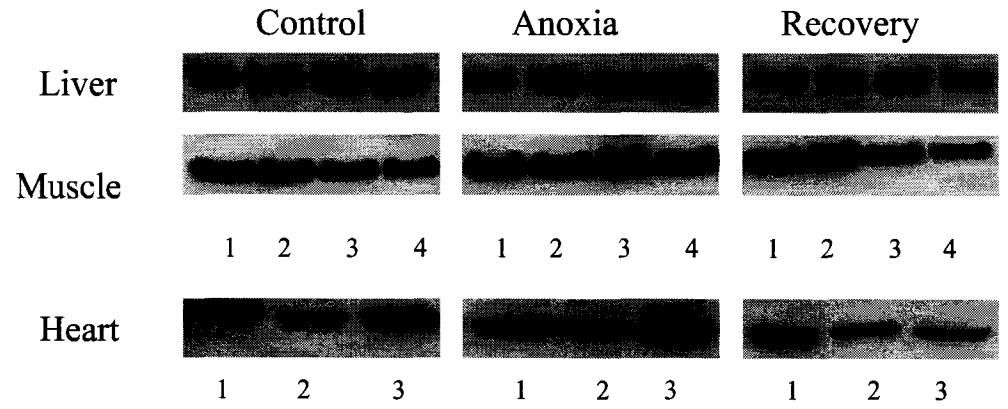

(B)

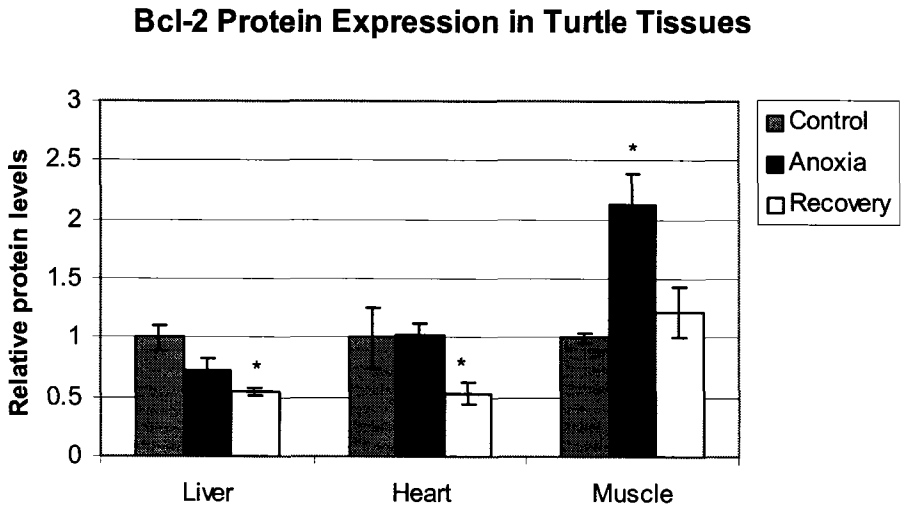

Figure 3.8 Protein expression of phospho-Bcl-2 (Ser70) in three tissues of red-eared slider turtles. **(A)** Representative Western blots showing the phospho-Bcl-2 (Ser70) protein band at ~30 kDa in tissues of control, anoxic and recovered turtles. Protein bands were normalized against Coomassie stained bands. **(B)** Histograms showing the relative phospho-Bcl-2 (Ser70) protein levels in turtle tissues. Data are mean ± SEM, n= 3 independent trials. * - Values for anoxic or recovery samples are significantly different from the corresponding control values using the two-tailed Student's *t*-test, $P < 0.05$.

Figure 3.8

(A)

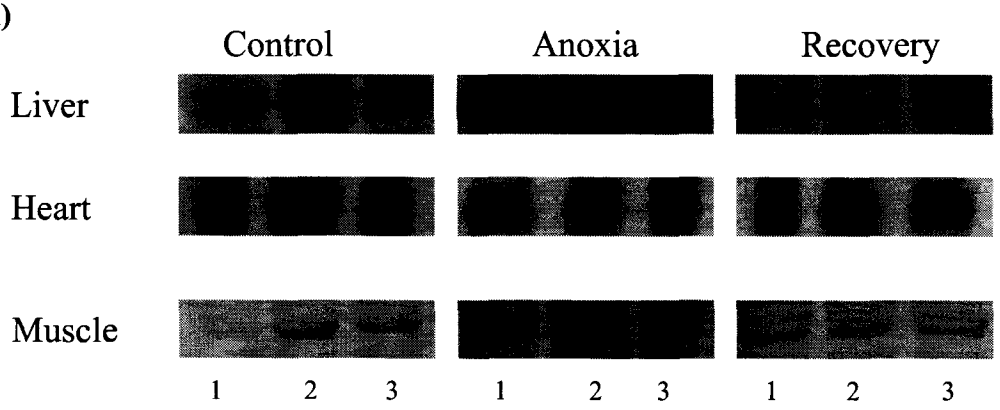

(B)

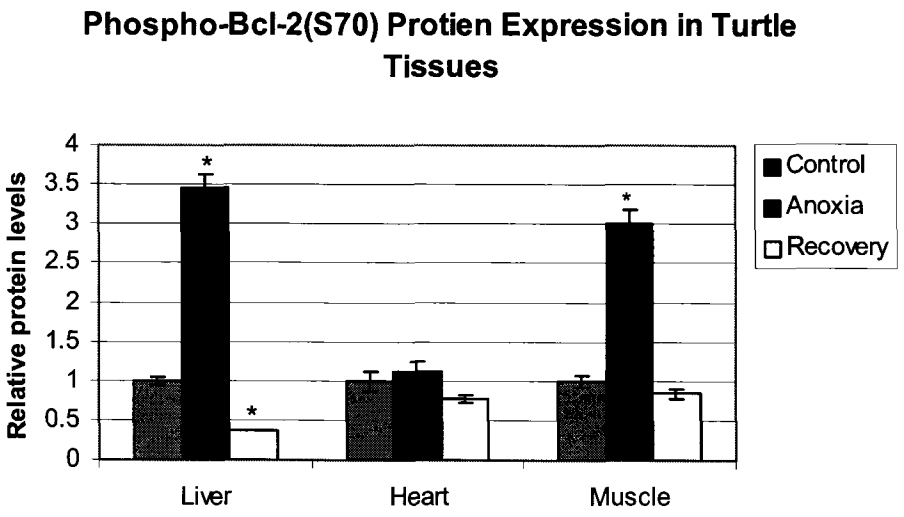

Figure 3.9 Mcl-1 protein expression in four tissues of red-eared slider turtles. **(A)** Representative Western blots showing the Mcl-1 protein band at ~40 kDa in tissues of control, anoxic and recovered turtles. Protein bands were normalized against Coomassie stained bands. **(B)** Histograms showing the relative Mcl-1 protein levels in turtle tissues. Data are mean ± SEM, n= 4 independent trials for liver and kidney and n=3 for heart and skeletal muscle. * - Values for anoxic or recovery samples are significantly different from the corresponding control values using the two-tailed Student's *t*-test, $P < 0.05$.

Figure 3.9

(A)

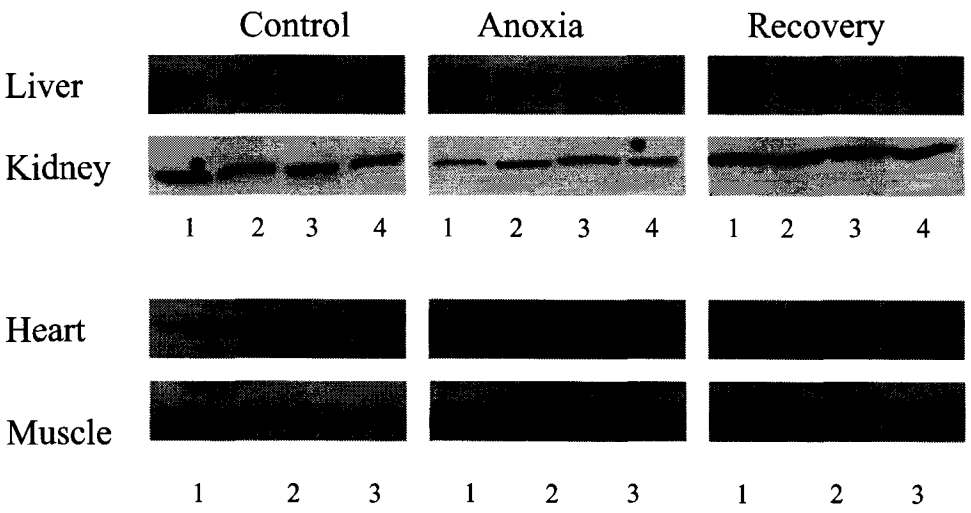

(B)

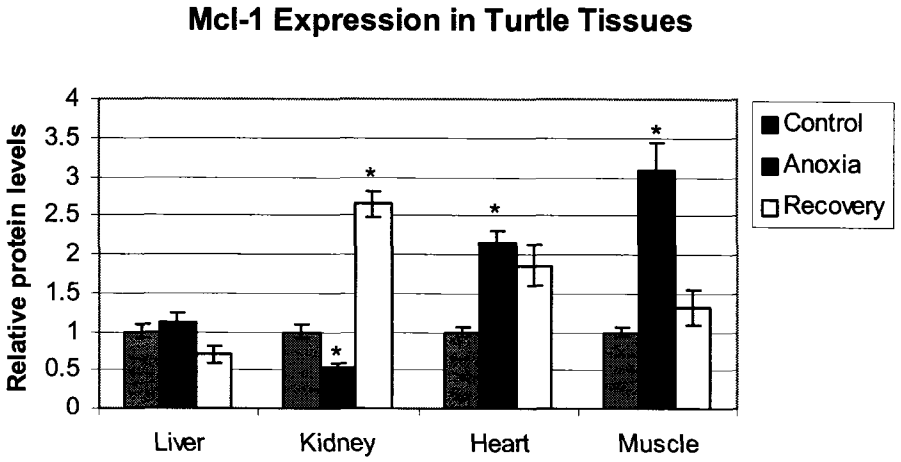

Figure 3.10 Protein expression of phospho-Bad (Ser112) in three tissues of red-eared slider turtles. **(A)** Representative Western blots showing the phospho-Bad (Ser112) protein band at ~30 kDa in tissues of control, anoxic and recovered turtles. Protein bands were normalized against Coomassie stained bands. **(B)** Histograms showing the relative phospho-Bad (Ser112) protein levels in turtle tissues. Data are mean ± SEM, n= 4 independent trials. * - Values for anoxic or recovery samples are significantly different from the corresponding control values using the two-tailed Student's *t*-test, $P < 0.05$.

Figure 3.10

(A)

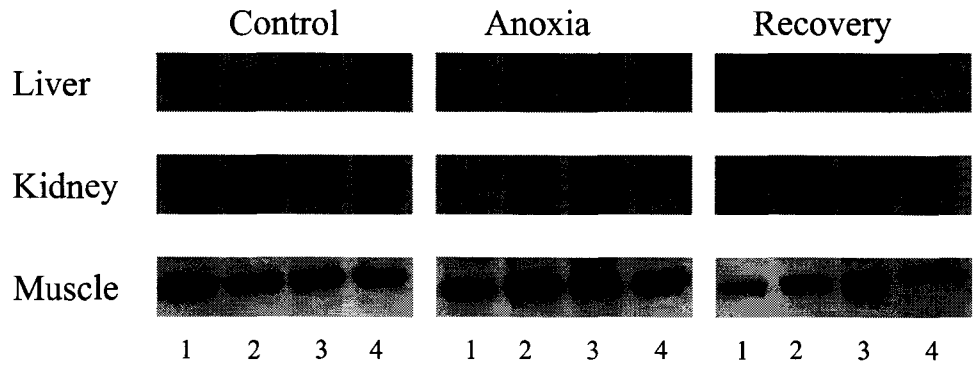

(B)

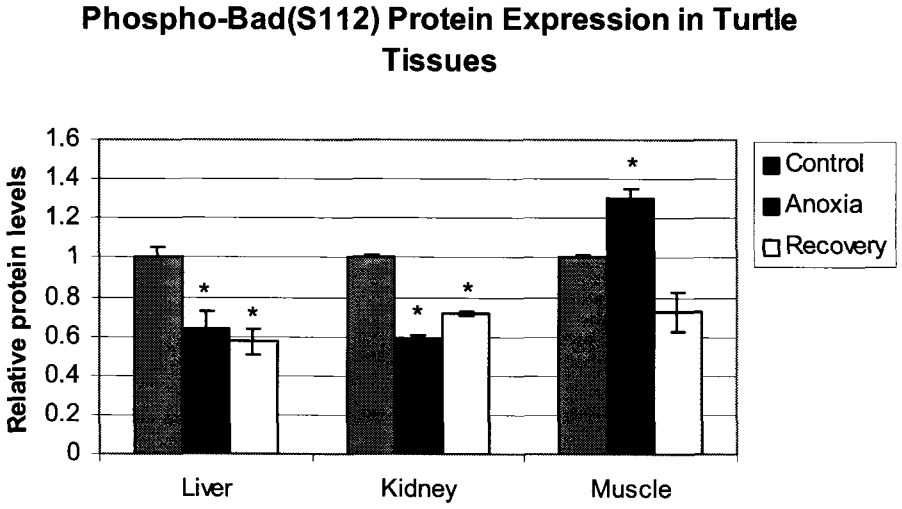

Discussion

Apoptosis can be induced by a wide array of death signals such as anoxia and oxidative stress in species that are not tolerant of these stresses. However, tissues of anoxia tolerant turtles undergo repeated bouts of anoxia and reoxygenation without encountering apparent injury and apoptosis. The mechanisms underlying antiapoptotic regulation in anoxia tolerant turtles during anoxia and the following aerobic recovery were unknown prior to the present study. Studies of mechanisms of apoptotic regulation in mammals have suggested that modulation of the levels of Bcl-2 family members plays an important role in controlling cell fate. For example, according to Parsadanian *et al.* (1998), Bcl-X_L overexpression was neuroprotective with substantially enhanced neuron survival in the hippocampus of hypoxia-ischemia treated mice. Saitoh *et al.* (2003) reported that up-regulation of Bcl-2 protein prevented hypoxia/reoxygenation-induced cell death in rat fibroblastic cells. Thus, growing evidence has suggested that enhanced protein expression of antiapoptotic members of Bcl-2 protein family delays or blocks apoptosis in a variety of cells in response to stress stimuli. On the other hand, loss-of-function analysis revealed that Bcl-2-deficient mice displayed apoptosis of lymphocytes and developmental renal cell death (Veis *et al.*, 1993). Apoptotic stimuli, such as DNA damage, lead to increased expression of proapoptotic family members (Petros *et al.*, 2004). Furthermore, covalent modification by protein phosphorylation alters anti or pro apoptotic activities and interactions of Bcl-2 family proteins. For example, it has been shown that phosphorylation of the proapoptotic protein Bad at serine

112 results in its sequestration in the cytosol which prevents it from interacting with Bcl-X_L and Bcl-2 at the mitochondrial membrane, and thus inhibits the proapoptotic actions of the Bad protein (Zha *et al.,* 1996; Tan *et al.,* 2000).

Bcl-X_L protein belongs to the antiapoptotic members of the Bcl-2 protein family, which protect cells against a broad range of apoptotic stimuli. In this chapter, the *bcl-xl* gene sequence from *T. s. elegans* white muscle was partially cloned. Analysis of the *bcl-xl* nucleotide and putative amino acid sequences demonstrated that turtle *bcl-xl* shares high identity with the isoform from chicken (79% nucleotide identity and 68% amino acid identity), but relatively low identity with mammalian species such as house mouse and pig (66% nucleotide identity and 57% amino acid identity).

Previous structural analysis of the Bcl-2 family in mammals has demonstrated that the Bcl-X_L protein contains regions of similarity to other Bcl-2 family proteins, termed Bcl-2 homology (BH) 1-4 domains (Danial and Korsmeyer, 2004). BH domains are short alpha-helix motifs which mediate protein:protein interactions between Bcl-2 family proteins and are important for apoptosis regulation (Gross *et al.*, 1999). Indeed, the structure of a mammalian Bcl-X_L monomer revealed that its BH1, BH2, and BH3 domains were in close proximity and created a hydrophobic pocket which could accommodate a BH3 domain of a proapoptotic member such as Bad (Muchmore *et al.*, 1996; Danial and Korsmeyer, 2004). Unfortunately, the amplified fragment of turtle Bcl-X_L did not include the BH1, BH2 or BH4 domains so it was impossible to tell if these domains were different in the anoxia tolerant turtle. Nevertheless, the BH3

conserved domain was identified with the sequence LREAGDEFEL (Figure 3.4A, in **bold underline**) when the partial turtle Bcl-X_L amino acid sequence was compared to Bcl-X_L sequences from mammals. The amino acid sequence alignment of Bcl-X_L shows that the BH3 domain of turtle Bcl-X_L is strictly conserved without amino acids substitutions as compared with the mammalian sequence and with only one difference compared with chicken. Therefore, the highly conserved BH3 region in turtle Bcl-X_L may exert the same biological functions as it does in other species, in that the BH3 region of Bcl-X_L is mainly responsible for mediating interactions with proapoptotic proteins (Petros *et al.*, 2004).

Signaling pathways that regulate apoptosis can directly alter the expression of Bcl-2 family members at both the transcriptional and translational levels (Adams and Cooper, 2007). Our results for relative RT-PCR and Western blots show that mRNA expression levels and protein levels of Bcl-X_L are differently regulated in heart of anoxia tolerant turtles. Specifically, in heart, Bcl-X_L protein levels increased during anoxia by 1.41-fold over controls and returned to control levels following recovery. Therefore, elevated Bcl-xL levels may play a role to protect turtle heart cells, rising during anoxia to help prevent cells from undergoing apoptosis. Interestingly, Bcl-X_L transcript levels in heart decreased significantly during anoxia and, hence, did not correlate with the elevated Bcl-X_L protein levels. These data provide evidence that mRNA expression is not necessarily coordinately regulated with protein levels and that the protein level of Bcl-X_L could be controlled by posttranscriptional or posttranslational regulation in heart in

response to anoxic treatment. Specifically, in addition to mRNA substrate availability, mRNA stability also contributes to the expression pattern of a gene. The more stable the mRNA, the greater the number of proteins produced from any one transcript. Moreover, net protein content is governed by the rates of both protein synthesis and protein degradation and it is possible that reduced degradation of selected proteins could enhance their net levels in anoxia (Storey and Storey, 2004). Indeed, studies have shown that compared with controls, the half-life of the labile protein pool increased by 40% in when hepatocytes of anoxia-tolerant painted turtles (*C. p. bellii*) were exposed to anoxia (Land and Hochachka, 1994; Storey and Storey, 2004). Another likely mechanism that could account for the elevation of Bcl-X_L protein levels in turtle heart in anoxia was suggested by a recent paper that showed that *bcl-xl* mRNA contains an internal ribosome entry site (IRES) (Yoon *et al.*, 2006). Stress conditions typically halt the translation of most mRNA species, those that are processed by so-called cap-dependent translation but about 3-5% of cell proteins possess an IRES that allows their continued translation under energy-limiting conditions (Holcik and Sonenberg, 2005). A number of well-known stress responsive proteins contain an IRES including HIF-1alpha, GRP78, and XIAP (another anti-apoptosis protein). Thus, the presence of an IRES in *bcl-xl* mRNA probably ensures its enhanced translation in anoxia and suggests its probable importance for apoptosis inhibition and sustained viability under anoxia. Expression levels of Bcl-X_L were also measured in white muscle of control, anoxia and recovery turtles. Protein content remained constant during anoxia and recovery in muscle indicating that Bcl-X_L

may not be as important to antiapoptotic defense in skeletal muscle.

Mcl-1 is another antiapoptotic Bcl-2 family member that acts as an important molecule in apoptosis control, promoting cell survival by interfering at an early stage in a cascade of events leading to release of cytochrome c from mitochondria (Michels *et al.*, 2005). The localization of Mcl-1 in the outer mitochondrial membrane is consistent with its role in controlling key mitochondrial events during apoptosis (Yang *et al.*, 1995). In this chapter, Western blotting showed that the protein content of Mcl-1 increased significantly during anoxia and returned to control levels during recovery in heart and skeletal muscle of anoxia tolerant turtles. Indeed, maintenance or overexpression of Mcl-1 levels blocks apoptosis in a wide range of cell types (Adams and Cooper, 2007). Meanwhile, loss of Mcl-1 has been shown to play a key role in apoptosis induced by various death stimuli such as UV irradiation and viral infection (Nijhawan *et al.*, 2003; Rahmani *et al.*, 2005). Hence, our data are consistent with the notion that the elevated levels of Mcl-1 possibly provide hearts and muscles of anoxia tolerant turtles with anti-apoptotic defense in response to anoxia. Mcl-1Different expression patterns of Mcl-1 were observed in liver and kidney. Liver showed unchanged levels of Mcl-1. Perhaps other antiapoptotic members may compensate for the stable levels of Mcl-1 in turtle liver. Alternatively, maintenance of Mcl-1 levels in turtle liver may be already sufficient to protect liver cells from anoxia-induced apoptosis. In kidney, Mcl-1 decreased by 46% during anoxia followed by a significant increase above control levels during recovery. Mcl-1 is rapidly degraded in response to cell death signals and is immediately re-induced

by survival stimuli (Fang and Yen, 2006) and this may be what occurred in turtle kidney, re-oxidation triggering a rapid resynthesis of the protein. Adams and Copper (2007) observed that rapid turnover of Mcl-1 couples translation to cell survival and apoptosis. Thus, the rapid change of Mcl-1 levels during anoxia and recovery in turtle kidney may suggest that there was a transition of overall environment from apoptosis to cell survival, although evidence shows that down-regulation of Mcl-1 alone is not sufficient to disrupt mitochondrial integrity and promote apoptosis (Fritsch *et al.*, 2007).

The amount of Bcl-2 protein and its relative phosphorylation state, as judged by phospho-Bcl-2 (Ser70) content, showed different patterns (Figure 3.7 and Figure 3.8) in the three organs tested (liver, heart and skeletal muscle). In heart, the data indicate that both the total content and phosphorylation state of Bcl-2 were unchanged. Total Bcl-2 levels remained stable in liver during anoxia but the amount of phosphoprotein increased during anoxia. A similar expression pattern was seen in muscle, in which both the overall Bcl-2 protein and its phosphorylated form were up-regulated during anoxia. Over-expression of Bcl-2 has been shown to enhance survival of mammalian cells in response to various stimuli (Figueroa *et al.*, 2001; Mastrangelo *et al.*, 2000). Furthermore, emerging evidence suggests that phosphorylation of Bcl-2 enforces its antiapoptotic function, which may affect its capacity for dimerization with other proapoptotic proteins and/or its stability (Huang and Cidlowski, 2002). Hence, enhanced levels of phospho-Bcl-2 (Ser70) in both muscle and liver may be necessary to allow this protein to inhibit anoxia-induced apoptosis. By contrast, the opposite expression pattern was

observed in liver during aerobic recovery with reduced protein levels of both the total Bcl-2 protein and its phosphorylated form. Hence, it is possible that other antiapoptotic signaling pathways and antiapoptotic molecules such as NF-kappa B or the cellular inhibitor of apoptosis (cIAP) might be activated and enhanced during recovery to promote liver cell survival (Kim *et al.*, 2007; Chua *et al.*, 2007).

Bad, a proapoptotic member of the Bcl-2 family, is a critical regulatory component of the intrinsic cell death machinery that exerts its death-promoting effect upon heterodimerization with the antiapoptotic proteins Bcl-2 and Bcl-X_L (Schürmann *et al.*, 2000). Phosphorylation of Bad at different residues blocks its apoptotic activity modulated through different mechanisms. For example, phosphorylation of Ser 112 and Ser 136 leads to sequestering of Bad by cytosolic 14-3-3-family proteins whereas phosphorylation at Ser 155 leads to a conformational change in the Bad protein that blocks its binding to Bcl-X_L (Hirai and Wang, 2001). Phospho-Bad (Ser112) content was measured in three tissues of anoxia tolerant turtles but antibodies recognizing phospho-Bad (Ser 136) and phospho-Bad (Ser155) did not crossreact with the turtle protein. In muscle, phosphorylation at the Ser 112 site increased strongly during anoxia (Figure 3.10), which suggests that the action of the proapoptotic protein Bad is suppressed in muscle by the enhanced phosphorylation during anoxia. When combined with the data showing elevated expression levels of antiapoptotic proteins such as Mcl-1 and Bcl-2 in muscle during anoxia, this suggests an overall balance in favor of anti-apoptotic signaling in the muscle of the anoxia tolerant turtle. By contrast,

anoxia/recovery had opposite effects on the phosphorylation state of Bad in liver and kidney; the content of phospho-Bad Ser 112 being reduced during anoxia and recovery. Hence, pro-apoptotic signaling could be enhanced in liver and kidney during anoxia and recovery but further study of the changes in the ratios of Bad and other antiapoptotic proteins levels is required to determine whether cells will be protected from apoptosis in anoxia or might die from it.

The expression of several pro-survival and/or apoptotic genes is an important aspect of cell fate regulation. The overall data in this chapter for members of Bcl-2 protein family (Bcl-X_L, Mcl-1, Bcl-2 and p-Bad) show that anti- and pro-apoptotic proteins do have their own, tissue-specific response patterns in anoxia tolerant turtles. Indeed, it has also been determined from analysis of the phenotype of bcl-2-/- knockout mice that different cell types may have their own specific apoptosis regulation. These mice develop normally, with apoptosis occurring only in some tissues and organs and not in others (Veis *et al.*, 1993; Kamada *et al.*, 1995). Furthermore, the ratio between the anti-apoptotic proteins and the pro-apoptotic proteins dictates the sensitivity of a cell to a death signal (Gross *et al.*, 1999; Zha *et al.*, 1996). For example, a previous study found that the ratio of mRNA for the expression of the proapoptotic gene Bax and the antiapoptotic gene Bcl-2 increased significantly in the human oviduct tissue in cells undergoing apoptosis (Briton-Jones *et al.*, 2006).

In conclusion, the current study provides evidence that potent anti-apoptotic proteins in the Bcl-2 family (Bcl-X_L, Mcl-1, Bcl-2) may play a positive role in the

response to anoxia and/or recovery with increased expression in selected tissues of anoxia tolerant *T. s. elegans*. In addition, the enhanced phosphorylation of Bad protein at the serine 112 site in muscle possibly reflects the pro-apoptotic activity of Bad is inhibited in muscle during anoxia. Overall, these results suggest that cellular mechanisms of apoptosis were suppressed during anoxia or aerobic recovery. Future studies should examine the responses of other anti- and pro-apoptotic proteins in turtle organs under oxygen stress as well as investigate the actual changes in the ratio of anti- and pro-apoptotic protein expression levels.

Chapter 4
General Discussion

The red-eared slider turtle (*Trachemys scripta elegans*) has been extensively used as a good model in which to study the adaptations needed by vertebrate organs for anoxia tolerance and for dealing with hypoxia/reoxygenation (Storey, 2007; Willmore *et al.*, 2001; Willmore and Storey, 1997a). This turtle is able to survive submerged under water all winter in water in that may be ice-covered without oxygen for several months and little or no ability to take oxygen from the water across various body surfaces. Moreover, after prolonged hypoxic/anoxic submergence, the resumption of aerial breathing results in a sudden reintroduction of oxygen into the turtle body which could create a potential danger of ROS overproduction and oxidative damage to tissues. Therefore, a natural life style of repeated bouts of deoxygenation and reoxygenation makes red-eared slider turtles face at least two serious consequences for cells and tissues: (1) Oxidative damage caused by oxidative stress could occur when turtle tissues undergo cycles of hypoxia/anoxia and reoxygenation, (2) Apoptosis is often triggered by oxygen deprivation and oxidative stress. Turtles must have developed effective ways to deal with these stresses.

Studies of the molecular adaptations for hypoxia/anoxia and oxidative stress in red-eared slider turtles have suggested that stress-responsive gene expression may play an important role in the survival of these natural stresses. The first study to explore anoxia-induced gene expression in turtles used differential screening of a red-eared slider turtle heart cDNA library to identify several mitochondrial genes that were anoxia-upregulated (Cai and Storey, 1996). This study indicated that new types of transcripts or proteins may be produced to support turtle anoxia survival. The current

thesis further analyzed the biochemical adaptations at gene and protein levels via modern molecular biology techniques and highlighted multiple molecular adaptations to anoxia and oxidative stress in turtles including changes in gene expression, changes in protein levels, and altered subcellular localization of transcription factors.

The genes and proteins that were studied in my thesis belong to two general categories: those involved in antioxidant defense that deal with oxidative stress during anoxia/reoxygenation (Chapter two) and those involved in antiapoptotic defense to prevent cell death as a result of anoxia or oxidative stresses (Chapter three). Techniques of molecular biology including Western blotting and Semi-quantitative RT-PCR were used to examine the expression levels of multiple genes and proteins with key roles in antioxidant and antiapoptotic defenses (e.g. GSTs, Bcl-2 family proteins). In addition, the subcellular localization of a stress-induced transcription factor (Nrf2) in response to anoxia was also studied. Overall, the work presented demonstrated that differential expression of genes was involved in antioxidant and antiapoptotic defenses of the red-eared slider turtle. Furthermore, the results indicating the translocation of Nrf2 under anoxia exposure provided insights into the use of transcription factors to activate the transcription of certain downstream genes, whose protein products support natural stress survival in anoxia tolerant turtles.

Antioxidant gene regulation in the red-eared slider turtle

The protein expression of mitochondrial superoxide dismutase (Mn SOD) was

upregulated both in heart and muscle of anoxia-exposed turtles whereas its expression did not change in liver and kidney under anoxia exposure. Because of its mitochondrial location, Mn SOD is believed to be the principal defense against the toxicity of O_2^- generated by the oxidative phosphorylation in the mitochondrial matrix (Martin, 2006). Hypoxia/anoxia and reoxygenation may disturb the ability of the cell to sequester O_2^- in the mitochondrial matrix, and once the O_2^- level is beyond the capacity of the available Mn SOD activity, it may move out into the cytosol where the main oxidative damage is initiated (Park et al., 1998). Overexpression of the Mn SOD gene to enhance Mn SOD protein levels would then alleviate this problem. Elevated amounts of Mn SOD in turtle heart and muscle would offer a means of increasing the catalytic capacity for the dismutation of superoxide radicals that can leak from the electron transport chain of mitochondria during anoxia. Moreover, the generation of ROS is accelerated as an oxidative burst during reoxygenation since this stimulates the conversion of dehydrogenases to oxidases and the introduction of excess O_2^- into the cytoplasm (Park *et al.*, 1998). Therefore, the upregulation of Mn SOD during anoxia in turtle tissues could also serve as an anticipatory preparation and provide a rapid Mn SOD protein pool for decreasing the potential damage due to oxidative stress during reoxygenation.

Another group of antioxidant enzymes, four GST isozymes (GSTK1, GSTP1, GSTT1 and GSTM3), were identified in turtle tissues. The results for GSTs provide evidence that organ-specific changes in the amount or classes of GST isozymes occur under anoxia and/or recovery from anoxia in turtle tissues. Not every GST protein was

detected in every tissue, and each enzyme showed different patterns of response both between tissues and as compared with other family members in the same tissue. For instance, the protein levels of GSTK1 in kidney increased significantly during anoxia but GSTT1 levels remained stable. Increased levels of GSTs in selected tissues suggest the need for higher GST protein availability to maintain or enhance capacity for detoxifying oxidative damage products that accumulate during transitions between anoxic and aerobic states in organs. Furthermore, it has been shown that red-eared slider turtles rely upon high constitutive activities of antioxidant enzymes to deal with oxidative stress (Willmore and Storey, 1997b). Therefore, even though some GST levels were reduced or remained stable during anoxia and/or recovery in some turtle tissues, it is likely that the remaining levels would still be sufficient to protect turtle tissues from damage caused by ROS.

Remarkably, however, my data showed that protein contents of Mn SOD and all four GST isozymes were elevated under anoxia and/or reoxygenation in the skeletal muscle of the turtles. This might be explained by the muscle's need to minimize ROS production and resist muscle disuse atrophy during prolonged anoxic hibernation when the skeletal muscle of turtles would be largely inactive. In mammals and some frogs, muscle inactivity can result in atrophy, characterized by a reduction in muscle fibre cross-sectional area and a concomitant loss of muscle strength (Hudson and Franklin, 2002). It has been reported that disused skeletal muscle is particularly susceptible to oxidative damage as ROS escape into intracellular spaces from mitochondrial membranes (Kondo *et al.*, 1994). ROS have a significant degenerative effect on muscle fibers,

damaging muscle proteins and lipids and causing them to be degraded (Kondo et al., 1991). Thus, given the fact that anoxia tolerant turtles experience a dramatic reduction in skeletal muscle activity during winter hibernation, the upregulation of antioxidant enzymes such as Mn SOD and GSTs in turtle muscles provides a potent mechanism for reducing the production of ROS and limiting the potential for muscle disuse atrophy during anoxia/reoxygenation.

The stress-induced expression of antioxidant genes including *GSTs* and *Mn SOD* is commonly regulated by the transcription factor Nrf2. My data provide some evidence that Nrf2 might be responsible for the upregulation of GST and Mn SOD proteins in turtle tissues under anoxia, although it cannot exclude the involvement of other transcription factors or mechanisms of transcriptional regulation. The activation of Nrf2 under anoxia was supported by my data showing that more Nrf2 protein translocated to the nucleus from the cytoplasm under anoxic conditions compared with the aerobic control situation, particularly in liver and heart. This suggested the Nrf2 may be activated and involved in regulating antioxidant defense during anoxia/reoxygenation but further study is still needed to fully explore this regulatory mechanism.

Antiapoptotic gene regulation in the red-eared slider turtle

In the natural life of the red-eared slider, turtle organs are exposed to the dual challenges of oxygen-depleted environments resulting from breath-hold diving or prolonged hibernation under water and to oxidative environments resulting from the

generation of ROS particularly during aerobic recovery from anoxia when blood flow, oxygen delivery and oxygen consumption increase rapidly. Both anoxia and oxidative stress are known to induce mitochondria-dependent apoptosis in cells or tissues. Hence anoxia tolerant turtles need good antiapoptotic defense during anoxia and reoxygenation. In Chapter 3, the mitochondrial pathway of apoptosis was studied by analyzing mitochondrial proteins of the Bcl-2 family that have anti-apoptotic (Bcl-X_L, Bcl-2 and Mcl-1) versus pro-apoptotic (Bad) functions.

Data for Bcl-X_L showed that its mRNA levels decreased in heart under anoxia, but oppositely, its protein levels increased. This shows a lack of correlation between the mRNA and protein levels of a gene in anoxia tolerant turtles. In general, the availability of mRNA transcripts should be a primary determinant of protein levels. However, protein levels are also influenced by other regulatory mechanisms such as post-transcriptional processing of mRNA, differential mRNA stability, posttranslational modification of proteins, suppression of protein degradation, etc. (Storey and Storey, 2004). Indeed, under some unusual physiological conditions such as cellular stress (e.g. hypoxia, heat shock and oxidative stress) and apoptosis, regulation at the posttranslational level rather than the mRNA level allows for an immediate and rapid response to environmental changes (Holcik and Sonenberg, 2005). Furthermore, the evidence of the presence of an internal ribosome entry site (IRES) in *bcl-xl* mRNA may also explain the upregulated Bcl-X_L levels during anoxia in turtle heart. IRES-mediated protein translation during stress is controlled by the mechanism that ribosomes could selectively recruit certain mRNAs

through their IRES (Holcik and Sonenberg, 2005). Indeed, IRES-mediated protein translation occurs predominantly during apoptosis (Holcik and Sonenberg, 2005). Hence, it is likely that IRES-mediated translation is responsible for the enhanced levels of Bcl-X_L protein in anoxic turtle heart.

The data for other Bcl-2 family proteins showed organ-specific responses during anoxia and reoxygenation. Skeletal muscle showed enhanced expression of Bcl-2, phospho-Bcl-2 (Ser 70), Mcl-1 and phospho-Bad (Ser 112) proteins. Up-regulation and/or enhanced phosphorylation of these proteins is reported to protect cells or tissues from undergoing apoptosis (Piret *et al.*, 2005; Shimizu *et al.*; Huang *et al.*, 2002). Hence, my data suggests that antiapoptosis signals may dominate during anoxia and/or reoxygenation to promote cell survival in muscle. In heart, although Bcl-2 was down-regulated during anoxia, the up-regulation Mcl-1 in this organ might protect heart cells from apoptosis during anoxia/reoxygenation. The decreased levels of antiapoptotic proteins, Bcl-2 in liver and Mcl-1 in kidney as well as reduced levels of phospho-Bad (Ser 112) in both organs, indicates that anoxia/reoxygenation might trigger apoptotic signals in liver and kidney. However, it has been shown that cell fate decisions are influenced by the ratio between the antiapoptotic proteins and the proapoptotic proteins. Thus, further studies with levels of proapoptotic proteins in liver and kidney are necessary in order to test the possibility that proapoptotic signals are also decreased coordinately with these reduced antiapoptotic proteins in liver and kidney.

Outlook

The data presented in this thesis show that adaptive regulation of antioxidant and antiapoptotic defenses occurs in turtle tissues since selected genes/proteins are differentially expressed as a response to anoxia/reoxygenation in a tissue-specific manner. In addition, A ROS-sensitive transcription factor Nrf2 was activated during anoxia in selected tissues, which was also supported by elevated levels of antioxidant proteins that are known to be downstream targets of Nrf2.

Although this thesis demonstrated the differential expression of antioxidant and antiapoptotic genes and proteins in selected tissues of red-eared slider turtles, many questions remain unanswered. I demonstrated by Western blotting the translocation of Nrf2 from cytoplasm to nucleus during anoxia in some turtle tissues as well as the increased expression of proteins such as GST and Mn SOD whose genes are known targets of Nrf2. But transcript levels of *GST* and *Mn SOD* should also be analyzed via PCR in order to confirm whether or not the upregulation of these proteins is due to Nrf2-mediated transcriptional activation since other factors such as an anoxia-induced suppression of protein degradation could also contribute to the increased protein levels. Moreover, the antioxidant response element (ARE) is a *cis*-acting DNA regulatory element to which the activated Nrf2 binds and then starts the expression of antioxidant genes. Thus, further analyses of the binding activity of Nrf2 to the ARE promoter in control, anoxic and recovered turtles using electrophoretic mobility shift assay (EMSA) technology will be necessary in order to determine if the binding of Nrf2 with the ARE

increases during anoxia/reoxygenation and thereby stimulates ARE-dependent gene transcription.

This thesis also suggested that enhanced antiapoptotic defense plays a role in anoxia/reoxygenation tolerance in muscle. However, in liver and kidney, levels of various antiapoptotic proteins such as Bcl-2 and Mcl-1 strongly decreased. Therefore, it will be interesting to test the expression of other related proteins in antiapoptotic defense in these organs to determine if other antiapoptotic proteins such as NF-κB or cIAP are elevated to supplement the antiapoptotic response of Bcl-2 family proteins regulated via the mitochondrial pathway.

The activities of transcription factors are significant to regulating the expression of groups of proteins that protect cells from various stresses. Studies to date have shown that the transcription factor NF-κB, which can be activated by more than 150 different extracellular signals, may function generally as a central regulator of stress responses, since many forms of stressful conditions (e.g. irradiation, oxidative stress, ischemia/reperfusion, apoptosis, exposure to certain chemicals, etc.) all lead to NF-κB activation (Li and Stark, 2002). Multiple genes are transcriptionally upregulated by NF-κB including antiapoptotic genes such as cIAP proteins and Bcl-2 family members (Wang *et al.*, 1996; Wang *et al.*, 1999), and these have a close connection with antiapoptotic adaptations seen in the turtle during anoxia/reoxygenation stress. Therefore, it will be very meaningful to study the activation of NF-κB and identify the genes that are downstream targets of NF-κB during anoxia/reoxygenation in organs of red-eared slider

turtles. This further study would lead to a better understanding of molecular adaptations of anoxia tolerant turtles under natural anoxia and reoxygenation exposures.

References

Adams KW, Cooper GM. (2007) Rapid turnover of Mcl-1 couples translation to cell survival and apoptosis. *J. Biol. Chem.* 282: 6192-6200.

Berhane K, Widersten M, Engstrom A, Kozarich JW, Mannervik B. (1994) Detoxication of base propenals and other alpha, beta-unsaturated aldehyde products of radical reactions and lipid peroxidation by human glutathione transferases. *Proc. Natl. Acad. Sci. U.S.A.* 91(4): 1480-1484.

Blokhnia O, Virolainen E, Fagerstedt K. (2003) Antioxidants, oxidative damage and oxygen deprivation stress: a review. *Ann. Bot.* 91: 179-194.

Briton-Jones C, Lok IH, Po ALS, Cheung CK, Chiu TTY, Haines C. (2006) Changes in the ratio of Bax and Bcl-2 mRNA expression and their cellular localization throughout the ovulatory cycle in the human oviduct. *J. Assist. Reprod. Genet.* 23: 149-156.

Brooks SPJ, Storey KB. (1988) Anoxic brain function: molecular mechanisms of metabolic depression. *FEBS Lett.* 232: 214–216.

Brunelle JK, Chandel NS. (2002) Oxygen deprivation induced cell death: An update. *Apoptosis* 7: 475-482.

Buck LT, Pamenter ME. (2006) Adaptive responses of vertebrate neurons to anoxia – Matching supply to demand. *Respir. Physiol. Neurobiol.* 154: 226-240.

Cai Q, Storey KB. (1996) Anoxia-induced gene expression in turtle heart: upregulation of mitochondrial genes for NADH-ubiquinone oxidoreductase subunit 5 and

cytochrome C oxidase subunit 1. *Eur. J. Biochem.* 241: 83–92.

Chanas SA, Jiang Q, McMahon M, McWalter GK, McLellan LI, Elcombe CR, Henderson CJ, Wolf CR, Moffat GJ, Itoh K, Yamamoto M, Hayes JD. (2002) Loss of the Nrf2 transcription factor causes a marked reduction in constitutive and inducible expression of the glutathione S-transferase Gsta1, Gsta2, Gstm1, Gstm2, Gstm3 and Gstm4 genes in the livers of male and female mice. *Biochem. J.* 365: 405-416.

Chávez JC, Agani F, Pichiule P, LaManna JC. (2000) Expression of hypoxia-inducible factor-1alpha in the brain of rats during chronic hypoxia. *J. Appl. Physiol.* 89(5): 1937-1942.

Chua CC, Gao J, Ho YS, Xiong Y, Xu X, Chen Z, Hamdy RC, Chua BH. (2007) Overexpression of IAP-2 attenuates apoptosis and protects against myocardial ischemia/reperfusion injury in transgenic mice. *Biochim. Biophys. Acta* 1773: 557-583.

Cowan, KJ. (2004) The mitochondria: powerhouse of the cell. *In:* Functional Metabolism: Regulation and Adaptation (Storey KB, eds.) Wiley-Liss, Hoboken, NJ, pp. 211-241.

Crawford DR, Suzuki T, Davies KJA. (2000) Redox regulation of gene expression. In: Antioxidant and redox regulation of genes (Sen CK, Sies H, Baeuerle PS, Eds.). Academic Press, San Diego, pp. 21-45.

Cullinan SB, Diehl JA. (2006) Coordination of ER and oxidative stress signaling: The

PERK/Nrf2 signaling pathway. *Int. J. Biochem. Cell Biol.* 38: 317-332.

Danial NN, Korsmeyer SJ. (2004) Cell death: critical control points. *Cell* 116: 205-219.

Deng X, Gao F, Flagg T, May WSJ. (2004) Mono- and multisite phosphorylation enhances Bcl2's antiapoptotic function and inhibition of cell cycle entry functions. *Pro. Natl. Acad. Sci. USA.* 6: 153-158.

Dong Z, Venkatachalam MA, Wang J, Patel Y, Saikumar P, Semenza GL, Force T, Nishiyama J. (2001) Up-regulation of apoptosis inhibitory protein IAP-2 by hypoxia. Hif-1-independent mechanisms. *J. Biol. Chem.* 276 (22): 18702-18709.

Ernst CH. (1990) Systematics, taxonomy, variation, and geographic distribution of the slider turtle. In: Life History and Ecology of the Slider Turtle (Gibbons JB, Ed.), Smithsonian Institute Press, Washington DC, pp. 3–18.

Fang H, Yen Y. (2006) Mcl-1: a highly regulated cell death and survival controller. *J. Biomed. Sci.* 13: 201-204.

Figueroa B, Sauerwald TM, Mastrangelo AJ, Hardwick JM, Betenbaugh MJ (2001) Comparison of Bcl-2 to a Bcl-2 deletion mutant for mammalian cells exposed to culture insults. *Biotechnol. Bioeng.* 73(3): 211-222.

Fraser KPP, Houlihan DF, Lutz PL, Leone-Kabler S, Manuel L, Brechin JG. (2001) Complete suppression of protein synthesis during anoxia with no post-anoxia protein synthesis debt in the red-eared slider turtle *Trachemys scripta elegans. J. Exp. Biol.* 204: 4353-4360.

Fridovich I. (1995) Superoxide radical and superoxide dismutases. *Annu. Rev. Biochem.*

64: 97-112.

Fritsch RM, Schneider G; Saur D, Scheibel M, Schmid RM. (2007) Translational repression of Mcl-1 couples stress-induced eIF2α phosphorylation to mitochondrial apoptosis initiation. *J. Biol. Chem.* In press; Epub Jun 6, 2007.

Giudice A, Montella M. (2006) Activation of the Nrf2-ARE signaling pathway: a promising strategy in cancer prevention. *BioEssays* 28:169-181.

Gnaiger E, Mendez G, Hand SC. (2000) High phosphorylation efficiency and depression of uncoupled respiration in mitochondria under hypoxia. *Proc. Natl. Acad. Sci. U.S.A.* 97(20): 11080-11085.

Gross A, Mcdonnell JM, Korsmeyer SJ. (1999) Bcl-2 family members and the mitochondria in apoptosis. *Gene Devel.* 13: 1899-1911

Gupta S. (2001) Molecular steps of death receptor and mitochondrial pathways of apoptosis. *Life Sci.* 69: 2957-2954.

Halliwell B, Gutteridge JMC. (1999) Free radicals in biology and medicine, Oxford University Press, Oxford, U.K.

Hasan Z, Ashraf M, Tayyebi A, Hussain R. (2006) *M. leprae* inhibits apoptosis in THP-1 cells by downregulation of Bad and Bak and upregulation of Mcl-1 gene expression. *BMC Microbiol.*6: 78.

Hawkins AJS. (1991) Protein turnover: a functional appraisal. *Funct. Ecol.* 5: 222–233.

Hayes JD, Ellis EM, Neal GE, Harrison DJ, Manson MM. (1999) Cellular response to cancer chemopreventive agents: Contribution of the antioxidant responsive

element to the adaptive response to oxidative and chemical stress. *Biochem. Soc. Symp.* 64: 141-168.

Hayes JD, Pulford DJ. (1995) The glutathione S-transferase supergene family: regulation of GST and the contribution of the isoenzymes to cancer chemoprotection and drug resistance. *Crit. Rev. Biochem. Mol. Biol.* 30(6): 445-600.

He SQ, Zhang YH, Venugopal SK, Dicus CW, Perez RV, Ramsamooj R, Nantz MH, Zern MA, Wu J. (2006) Delivery of antioxidative enzyme genes protects against ischemia/reperfusion-induced liver injury in mice. *Liver. Transpl.* 12: 1869-1879.

Hermes-Lima M, Storey JM, Storey KB. (2001) Antioxidant defenses and animal adaptation to oxygen availability during environmental stress. In: Cell and Molecular Responses to Stress (Storey KB, Storey JM, Eds.), Elsevier Press, Amsterdam, Vol. 2, pp. 263-287.

Hirai I, Wang HG. (2001) Survival-factor-induced phosphorylation of Bad results in its dissociation from Bcl-X_L but not Bcl-2. *Biochem. J.* 359: 345-352.

Hochachka PW, Lutz PL. (2001) Mechanism, origin, and evolution of anoxia tolerance in animals. *Comp. Biochem. Physiol.* 130: 435–459.

Holcik M, Sonenberg N. (2005) Translational control in stress and apoptosis. *Nature.* 6: 318-327.

Hollander J, Fiebig R, Gore M, Bejma J, Ookawara T, Ohno H, Ji LL. (1999) Superoxide dismutase gene expression in skeletal muscle: fiber-specific adaptation to endurance training. *Am. J. Physiol.* 277: 856-862.

Horiuchi M, Hayashida W, Kambe T, Yamada T, Dzau VJ. (1997) Angiotensin type 2 receptor dephosphorylates Bcl-2 by activating mitogen-activated protein kinase phosphatase-1 and induces apoptosis. *J. Biol. Chem.* 272: 19022-19026.

Huang STJ, Cidlowski JA. (2002) Phosphorylation status modulates Bcl-2 function during glucocorticoid-induced apoptosis in T lymphocytes. *FASEB J.* 16: 825-832.

Hudson NJ, Franklin CE. (2002) Maintaining muscle mass during extended disuse: aestivating frogs as a model species. *J. Exp. Biol.* 205:2297-303.

Hussain SP, Amstad P, He P, Robles A, Lupold S, Kaneko I, Ichimiya M, *et al.* (2004) p53-induced up-regulation of MnSOD and GPx but not catalase increases oxidative stress and apoptosis. *Adv. Cancer Res.* 64(7): 2350-2356.

Itoh K, Wakabayashi N, Katoh Y, Ishii T, Igarashi K, Engel JD, et al. (1999) Keap1 represses nuclear activation of antioxidant responsive elements by Nrf2 through binding to the amino-terminal Neh2 domain. *Genes Dev.*13 (1): 76-86.

Jackson DC. (1968) Metabolic depression and oxygen depletion in the diving turtle. *J. Appl. Physiol.* 24: 503-509.

Jackson DC. (2000) Living without oxygen: lessons from the freshwater turtle. *Comp. Biochem. Physiol. A* 125: 299-315.

Jang JH, Surh YJ. (2004) Bcl-2 attenuation of oxidative cell death is associated with up-regulation of gamma-glutamylcysteine ligase via constitutive NF-kappaB activation. *J. Biol. Chem.* 279(37): 38779-38786.

Janumyan YM, Sansam CG, Chattopadhyay A, Cheng N, Soucie EL, Penn LZ, Andrews

D, Knudson CM, Yang E. (2003). Bcl-XL/Bcl-2 coordinately regulates apoptosis, cell cycle arrest and cell cycle entry. *EMBO J.* 22: 5459-5470.

Ježek P, Hlavatá L. (2005) Mitochondria in homeostasis of reactive oxygen species in cell, tissues, and organism. *Int. J. Biochem. Cell Biol.* 37: 2478–2503.

Jones SP, Hoffmeyer MR, Sharp BR, Ho YS, Lefer DJ. (2003) Role of intracellular antioxidant enzymes after in vivo myocardial ischemia and reperfusion. *Am. J. Physiol.* 284(1): H277-H282.

Kakkar P, Singh BK. (2007) Mitochondria: a hub of redox activities and cellular distress control. *Mol.Cell. Biochem.* 12:913-922.

Kamada S, Shimono A, Shinto Y, Tsujimura T, Takahashi T, Noda T, *et al.* (1995) Bcl-2 deficiency in mice leads to pleiotropic abnormalities: accelerated lymphoid cell death in thymus and spleen, polycystic kidney, hair hypopigmentation, and distorted small intestine. *Cancer Res.* 55: 354-359.

Kang KW, Lee SJ, Park JW, Kim SG. (2002) Phosphatidylinositol 3-kinase regulates nuclear translocation of NF-E2-related factor 2 through actin rearrangment in response to oxidative stress. *Mol. Pharmacol.* 62 (5): 1001-1010.

Kerr JFR, Wyllie AH, Currie, AR. (1972) Apoptosis: a basic biological phenomenon with wide-ranging implications in tissue kinetics. *Br. J. Cancer.* 26: 239-257.

Kim S, Millet I, Kim HS, Kim JY, Han MS, Lee MK, Kim KW, Sherwin RS, Karin M, Lee MS. (2007) NF-kappa B prevents beta cell death and autoimmune diabetes in NOD mice. *Proc. Natl. Acad. Sci. U.S.A.* 104: 1913-1918.

Kluck RM, Bossy-Wetzel E, Green DR, Newmeyer DD. (1997). The release of cytochrome *c* from mitochondria: a primary site for Bcl-2 regulation of apoptosis. *Science* 275: 1132-1136.

Kobayashi A, Ito E, Toki T, Kogame K, Takahashi S, Igarashi K. (1999). Molecular cloning and functional characterization of a new Cap'n' collar family transcription factor Nrf3. *J. Biol. Chem.* 274(10): 6443-6452.

Kondo H, Nishino K, Itokawa Y. (1994) Hydroxyl radical generation in skeletal muscle atrophied by immobilization. *FEBS Lett.* 349(2): 169-172.

Kowluru RA, Kowluru V, Xiong Y, Ho YS. (2006) Overexpression of mitochondrial superoxide dismutase in mice protects the retina from diabetes-induced oxidative stress. *Free. Radic. Biol. Med.* 41(8): 1191-1196.

Land SC, Hochachka PW. (1994). Protein turnover during metabolic arrest in turtle hepatocytes: role and energy dependence of proteolysis. *Am. J. Physiol.* 266: C1028–C1036.

Li X, Stark GR. (2002) NFkappaB-dependent signaling pathways. *Exp. Hematol.* 30(4): 285-296.

Lushchak VI, Lushchak LP, Mota AA, Hermes-Lima M. (2001) Oxidative stress and antioxidant defenses in goldfish *Carassius auratus* during anoxia and reoxygenation. *Am. J. Physiol.* 280: R100-R107.

Lutz P L, Nilsson GE. (1997) The Brain without Oxygen. Austin, Texas: Landis Press: Chapman & Hall.

Lutz PL, Storey KB. (1997) Adaptations to variations in oxygen tension by vertebrates and invertebrates, *In:* Handbook of physiology, section 13: comparative physiology. (Dantzler WH, Ed.). Oxford Univ. Press, Oxford. pp. 1479-1522.

Magherini F, Tani C, Gamberi T, Caselli A, Bianchi L, Bini L, Modesti A. (2007) Protein expression profiles in *Saccharomyces cerevisiae* during apoptosis induced by H_2O_2. *Proteomics* 7: 1434-1445.

Mastrangelo AJ, Hardwick JM, Zou S, Betenbaugh MJ. (2000) Part II. Overexpression of bcl-2 families enhance survival of mammalian cells in response to various culture insults. *Biotechnol. Bioeng.* 67(5): 555-564.

McClintock DS, Santore MT, Lee VY, Brunelle J, Budinger GRS, *et al.* (2002) Bcl-2 family members and functional electron transport chain regulate oxygen deprivation-induced cell death. *Mol. Cell. Biol.* 22: 94-104.

McCord JM, Fridovich I. (1969) Superoxide dismutase. An enzymic function for erythrocuprein (hemocuprein). *J. Biol. Chem.* 244(22): 6049-6055.

Mehrani H, Storey KB. (1995). Enzymatic control of glycogenolysis during anoxic submergence in the freshwater turtle *Trachemys scripta. Int. J. Biochem. Cell Biol.* 27: 821–830.

Merighi S, Benini A, Mirandola P, Gessi S, Varani K, Leung E, Maclennan S, Baraldi PG, Borea PA. (2007) Hypoxia inhibits paclitaxel-induced apoptosis through adenosine-mediated phosphorylation of Bad in glioblastoma cells. *Mol. Pharmacol.* In press.

Michels J, Johnson PWM, Packham G. (2005) Molecules in focus Mcl-1. *Int. J. Biochem. Cell Biol.* 37: 262-271.

Milton SL, Prentice HM. (2007) Beyond anoxia: The physiology of metabolic downregulation and recovery in the anoxia-tolerant turtle. Comp. *Biochem. Physiol. A* 147(2): 277-290.

Milton SL, Nayak G, Lutz PL, Prentice HM. (2006) Gene transcription of neuroglobin is upregulated by hypoxia and anoxia in the brain of the anoxia-tolerant turtle *Trachemys scripta. J. Biomed. Sci.* 13(4): 509-514.

Motohashi H, Yamamoto M. (2004) Nrf2-Keap1 defines a physiologically important stress response mechanism. *Trends Mol. Med.* 10(11): 549-557.

Muchmore SW, Sattler M, Liang H, Meadows RP, Harian JE, Yoon HS, Nettesheim D, Chang BS, Thompson CB, Wong SL, Ng SH, Fesik SW. (1996) X-ray and NMR structure of human Bcl-X_L, an inhibitor of programmed cell death. *Nature.* 381: 335-341.

Nijhawan D, Fang M, Traer E, Zhong Q, Gao W, Du F, Wang X. (2003) Elimination of Mcl-1 is required for the initiation of apoptosis following ultraviolet irradiation. *Genes Dev.* 17: 1475–1486.

Nguyen T, Sherratt PJ, Pickett CB. (2003) Regulatory mechanisms controlling gene expression mediated by the antioxidant response element. *Annu. Rev. Pharmacol. Toxicol.* 43: 233-260.

Palacios-Callender M, Quintero M, Hollis VS, Springett RJ, Moncada S. (2004)

Endogenous NO regulates superoxide production at low oxygen concentrations by modifying the redox state of cytochrome c oxidase. *Proc. Natl. Acad. Sci. U.S.A.* 101(20): 7630-7635.

Park JI, Grant CM, Davies MJ, Dawes IW. (1998) The cytoplasmic Cu,Zn superoxide dismutase of *Saccharomyces cerevisiae* is required for resistance to freeze-thaw stress. Generation of free radicals during freezing and thawing. *J. Biol. Chem.* 273(36): 22921-22928.

Parsadanian AS, Cheng Y, Keller-Peck CR, Holtzman DM, Snider WD. (1998) Bcl-X_L is an anti-apoptotic regulator for postnatal CNS neurons. *J. Neurosci.* 18: 1009-1019.

Petros AM, Olejniczak ET, Fesik SW. (2004) Structural biology of the Bcl-2 family of proteins. *Biochim. Biophys. Acta* 1644: 83-94.

Piret JP, Minet E, Cosse JP, Ninane N, Debacq C, Raes M, Michiels C. (2005) Hypoxia-inducible factor-1-dependent overexpression of myeloid cell factor-1 protects hypoxic cells against *tert*-butyl hydroperoxide-induced apoptosis. *J. Biol. Chem.* 280: 9336-9344.

Prentice HM, Milton SL, Scheurle D, Lutz PL. (2004) The upregulation of cognate and inducible heat shock proteins in the anoxic turtle brain. *J. Cereb. Blood. Flow. Metab.* 24: 826–828.

Rahmani M, Davis EM, Bauer C, Dent P, Grant S. (2005) Apoptosis induced by the kinase inhibitor BAY 43-9006 in human leukemia cells involves down-regulation

of Mcl-1 through inhibition of translation. *J. Biol. Chem.* 280: 35217-35227.

Rushmore TH, Morton MR, Pickett CB. (1991) The antioxidant responsive element. activation by oxidative stress and identification of the DNA consensus sequence required for functional activity. *J. Biol. Chem.* 266(18): 11632-11639.

Rushmore TH, Pickett CB. (1993) Glutathione S-transferases: structure, regulation, and therapeutic implications. *J. Biol. Chem.* 268(16): 11475-11478.

Ruuge EK, Ledenev AN, Lakomkin VL, Konstantinov AA, Ksenzenko MY. (1991) Free radical metabolites in myocardium during ischemia and reperfusion. *Am. J. Physiol. Suppl.* 261: 81-86.

Saitoh Y, Ouchida R, Miwa N. (2003) Bcl-2 prevents hypoxia/reoxygenation-induced cell death through suppressed generation of reactive oxygen species and upregulation of Bcl-2 proteins. *J. Cell. Biochem.* 90: 914-924.

Sani M, Sebai H, Gadacha W, Boughattas NA, Reinberg A, Mossadok BA. (2006) Catalase activity and rhythmic patterns in mouse brain, kidney and liver. *Comp. Biochem. Physiol. B* 145(3-4): 331-337.

Schürmann A, Mooney AF, Sanders LC, Sells MA, Wang HG, Reed JC, Bokoch GM. (2000) p21-activated kinase 1 phosphorylates the death agonist Bad and protects cells from apoptosis. *Mol. Cell. Biol.* 20: 453-461.

Skulachev VP. (2000) Mitochondria in the programmed death phenomena; a principle of biology: " it is better to die than to be wrong". *IUBMB Life* 49: 365-373.

Stecyk JA, Farrell AP. (2007) Effects of extracellular changes on spontaneous heart rate

of normoxia- and anoxia-acclimated turtles (*Trachemys scripta*). *J. Exp. Biol.* 210: 421-431.

Storey KB. (1996) Metabolic adaptations supporting anoxia tolerance in reptiles: recent advances. *Comp. Biochem. Physiol. B.* 113: 23-35.

Storey KB. (2004) Molecular mechanisms of anoxia tolerance. *Int. Congr. Ser.* 1275: 47-54.

Storey KB. (2006a) Reptile freeze tolerance: metabolism and gene expression *Cryobiology* 52: 1–16.

Storey KB. (2006b) Gene hunting in hypoxia and exercise. *Adv. Exp. Med. Biol.* 588: 293-309.

Storey KB. (2007) Anoxia tolerance in turtles: Metabolic regulation and gene expression. *Comp. Biochem. Physiol. A.* 147: 263-276.

Storey KB, Storey JM. (1990) Facultative metabolic rate depression: molecular regulation and biochemical adaptation in anaerobiosis, hibernation and aestivation. *Q. Rev. Biol.* 65: 145-174.

Storey KB, Storey JM. (2004) Metabolic rate depression in animals: transcriptional and translational controls. *Biol. Rev.* 79: 207-233.

Takahashi A, Masuda A, Sun M, Centonze VE, Herman B. (2004) Oxidative stress-induced apoptosis is associated with alterations in mitochondrial caspase activity and Bcl-2-dependent alterations in mitochondrial pH (pH_m), *Brain Res. Bull.* 62: 497-504.

Tan YT, Demeter MR, Ruan H, Comb MJ. (2000) BAD Ser-155 phosphorylation regulates BAD/Bcl-XL interaction and cell survival. *J. Biol. Chem.* 275: 25865-25869.

Ultsch GR. (1989) Ecology and physiology of hibernation and overwintering among freshwater fishes turtles and snakes. *Bio. Rev.* 64: 435-516.

Vander HMG, Thompson CB. (1999) Bcl-2 proteins: regulators of apoptosis or of mitochondrial homeostasis? *Nat. Cell. Biol.* 1: E209-216.

Veis DJ, Sorenson CM, Shutter JR, Korsmeyer SJ. (1993) Bcl-2-deficient mice demonstrate fulminant lymphoid apoptosis, polycystic kidneys and hypopigmented hair. *Cel.* 75:229-240.

Wang CY, Guttridge DC, Mayo MW, Baldwin AS. (1999) NF-kappaB induces expression of the Bcl-2 homologue A1/Bfl-1 to preferentially suppress chemotherapy-induced apoptosis. *Mol. Cell. Biol.* 19(9): 5923-5929.

Wang CY, Mayo MW, Baldwin AS. (1996) TNF- and cancer therapy-induced apoptosis: potentiation by inhibition of NF-kappaB. *Science.* 274(5288): 784-787.

Warren DE, Reese SA, Jackson DC. (2006) Tissue glycogen and extracellular buffering limit the survival of red-eared slider turtles during anoxic submergence at 3 degrees C. *Physiol. Biochem. Zool.* 79(4): 736-744.

Wasser JS, Inman KC, Arendt EA, Lawler RG, Jackson DC. (1990) ^{31}P-NMR measurements of pHi and high energy phosphates in isolated turtle hearts during anoxia and acidosis. *Am. J. Physiol.* 259: 521–530.

Weisbrot-Lefkowitz M, Reuhl K, Perry B, Cahn PH, Inouye M, Mirochnitchenko O. (1998) Overexpression of human glutathione peroxidase protects transgenic mice against focal cerebral ischemia/reperfusion damage. *Molec. Brain. Res.* 53: 333-338.

Willmore WG, English TE, Storey KB. (2001) Mitochondrial gene responses to low oxygen stress in turtle organs. *Copeia* 2001(3): 628-637.

Willmore WG, Storey KB. (1997a) Antioxidant systems and anoxia tolerance in a freshwater turtle, *Trachemys scripta elegans*. *Mol. Cell. Biochem.* 170: 177-185.

Willmore WG, Storey KB. (1997b) Glutathione systems and anoxia tolerance in turtles. *Am. J. Physiol.* 273: R219-225.

Yang T, Kozopas KM, Craig RW. (1995) The intracellular distribution and pattern of expression of Mcl-1 overlap with, but are not identical to, those of Bcl-2. *J. Cell Biol.* 128: 1173–1184.

Yanada S, Saitoh Y, Kaneda Y, Miwa N. (2004) Cytoprotection by bcl-2 gene transfer against ischemic liver injuries together with repressed lipid peroxidation and increased ascorbic acid in livers and serum. *J. Cell. Biochem.* 93(5): 857-870.

Yoon A, Peng G, Brandenburg Y, Zollo O, Xu W, Rego E, Ruggero D. (2007) Impaired control of IRES-mediated translation in X-linked dyskeratosis congenital. *Science.* 312: 902-906.

Zha J, Harada H, Yang E, Jockel J, Korsmeyer SJ. (1996) Serine phosphorylation of death agonist BAD in response to survival factor results in binding to 14-3-3 not

Bcl-x(L). *Cell* 87: 619-628.

Appendix 1.

Antibodies tried in Western blotting but which did not cross-react with the corresponding proteins in red-eared slider turtle tissues

Proteins of interest	Primary antibodies tried	Source
GST T2	Rabbit anti-GST T2 polyclonal antibody	Gift from Dr. John Hayes, University of Dundee
GST A1	Rabbit anti-GST A1 polyclonal antibody	Gift from Dr. John Hayes, University of Dundee
GST A3	Rabbit anti-GST A3 polyclonal antibody	Gift from Dr. John Hayes, University of Dundee
GST A5	Rabbit anti-GST A5 polyclonal antibody	Gift from Dr. John Hayes, University of Dundee
GST M5	Rabbit anti-GSTM5 polyclonal antibody	Gift from Dr. John Hayes, University of Dundee
MafG	Rabbit anti-MafG polyclonal antibody	Biotechnology, Santa Cruz, CA
phospho c-Jun (Ser63)	Rabbit anti-phospho c-Jun (Ser63) polyclonal antibody	Cell Signaling, Technology, Inc. Beverly, MA
Heme oxygenase 1	Rabbit anti-HO-1 polyclonal antibody	Stressgen, Ann Arbor, MI
Bad	Rabbit anti-Bad polycolonal antibody	Cell Signaling, Technology, Inc. Beverly, MA
phospho-Bad (Ser136)	Rabbit anti-phospho-Bad (Ser136) polyclonal antibody	Cell Signaling, Technology, Inc. Beverly, MA
phospho-Bad (Ser155)	Rabbit anti-phospho-Bad (Ser155) polyclonal antibody	Cell Signaling, Technology, Inc. Beverly, MA